

# Origin and Early Differentiation of Carbon and Associated Life-Essential Volatile Elements on Earth

RAJDEEP DASGUPTA AND DAMANVEER S. GREWAL

## 2.1 Introduction

Earth's unique status as the only life-harboring planet in the inner Solar System is often linked to its orbit being in the habitable zone that resulted in the stabilization of liquid water on its surface. However, in addition to surface liquid water, the presence of carbon and other life-essential volatile elements (LEVEs) such as nitrogen and sulfur in the surface environment is also critical for the habitability of rocky planets. Earth's long-term equable climate and chemically habitable surface environment are therefore results of well-tuned fluxes of carbon and other LEVEs, involving the deep and the surficial Earth. Given that Earth developed into a volcano-tectonically active planet with both outgassing and ingassing mechanisms, the surface inventory of LEVEs over million- to billion-year timescales is maintained by interactions of the ocean–atmosphere system with the silicate fraction of the planet. Yet it remains uncertain how and when the initial inventory of LEVEs for the surface reservoir plus the silicate fraction (bulk silicate Earth (BSE) altogether), which set the initial boundary conditions for subsequent planet-scale volatile cycles, got established. The answers to these questions lie within Earth's formative years – in the building blocks, in the process of Earth's accretion, and in the early differentiation that made the major reservoirs that constitute the core, the mantle, and the crust–atmosphere.

Earth is a differentiated planet with a central metallic core and an outer shell of dominantly silicate rocks divided into the mantle and crust, which is overlain by the fluid envelope of the ocean–atmosphere system. Direct constraints on carbon and the other life-essential volatile abundance of Earth's core are lacking (Chapter 3, this volume), although significant concentrations of carbon, sulfur, hydrogen, and nitrogen can be in Earth's core given that the outer core is 10% lighter than pure Fe–Ni alloy liquid.<sup>1–3</sup> More is known about the carbon content of the present-day silicate fraction of the planet and its fluid envelope because Earth's mantle reservoir is sampled to some extent via mantle-derived melts (e.g. Refs. 4–9 and Chapter 9, this volume). Yet the estimates of bulk mantle carbon abundance from concentrations in basalts are uncertain partly because most basalts are partially degassed and basalt generation only directly samples typically the top 100–200 km of the mantle. Nonetheless, largely based on the carbon content of basalts (e.g.  $C/{}^3\text{He}$ ,  $\text{CO}_2/\text{Nb}$ ,  $\text{CO}_2/\text{Ba}$ , and  $C/{}^{40}\text{Ar}$  ratios), the BSE abundance of carbon is estimated to be

~100–530 ppm.<sup>7,9–13</sup> Among this range of estimated C budget for the BSE, most estimates<sup>7,9,10–12</sup> have converged to a concentration of 90–130 ppm, and this will be used in this chapter. It can be surmised that this BSE budget of C is an end product of Earth's accretion and early differentiation,<sup>8,14,16</sup> but the uncertainty in the C budget of BSE makes testing such hypotheses quantitatively less rigorous. Further insight could be gained, however, from C to other LEVE ratios (i.e. C/X, where X = N, S, or H; e.g. Refs. 7, 10, 11, 16–18). Specifically, these volatile ratios for the terrestrial reservoirs in general and BSE in particular could be compared with the same ratios in various planetary building blocks and evaluated against the known processes of planet formation and early differentiation.

The key questions focus on what planetary building blocks were responsible for delivering C and other associated LEVEs to Earth and when such delivery processes took place. If the C abundance and the C/X ratios of the BSE as well as the isotopic compositions of all LEVEs are similar to any of the undifferentiated meteorites, it may be concluded that such building blocks were responsible for bringing these volatiles to Earth and no postdelivery process altered their ratios (Figure 2.1). On the other hand, if the C abundance and C/X ratios of the BSE are distinct from these known building blocks, one needs to investigate whether any postdelivery processes could have altered these quantities such that the BSE LEVE geochemistry could be established. For example, if core formation processes fractionate C and/or affect the C/X ratios, then could equilibrium core formation scenarios be responsible for establishing carbon, oxygen, hydrogen, nitrogen, and sulfur in BSE (Figure 2.1)? The timing of volatile delivery is also important. If the LEVEs were delivered during the main stage of accretion, then early differentiation processes like core–mantle segregation and magma ocean (MO) degassing would have played an important role in setting up the relative budgets of the LEVEs in the primary reservoirs (Figure 2.1).<sup>8,11</sup> The delivery mechanism and the timing of delivery may be intimately linked; however, less interrogation has taken place thus far regarding the delivery mechanism. For example, there is a growing recognition that following an initial period of accretion of undifferentiated planetesimals, differentiated planetary embryos with masses ranging from ~0.01 to 0.1M<sub>E</sub> (where M<sub>E</sub> is the mass of present-day Earth) were abundant in the inner Solar System;<sup>19</sup> therefore, accretion of these differentiated bodies significantly contributed to the growth of larger planets like Earth.<sup>19,20</sup> Did the impacts or merger of differentiated bodies deliver the LEVEs to the BSE and establish the C abundance and the C/X ratios<sup>16,17</sup> or did post-core formation addition of undifferentiated or differentiated bodies<sup>21</sup> establish the BSE LEVE budget? And what were the relative contributions of the impacts of large differentiated and smaller undifferentiated bodies to bringing in LEVEs versus causing a depletion of LEVEs via atmospheric mass loss?<sup>22–24</sup>

This chapter will discuss the state of the art on what is known about the origin of C relative to the other LEVEs in the BSE, highlighting open questions and gaps in knowledge. We will discuss constraints based on geochemical comparison of the potential terrestrial building blocks with Earth reservoirs and interrogate each key process of planet formation and early differentiation, such as core formation, MO crystallization, MO

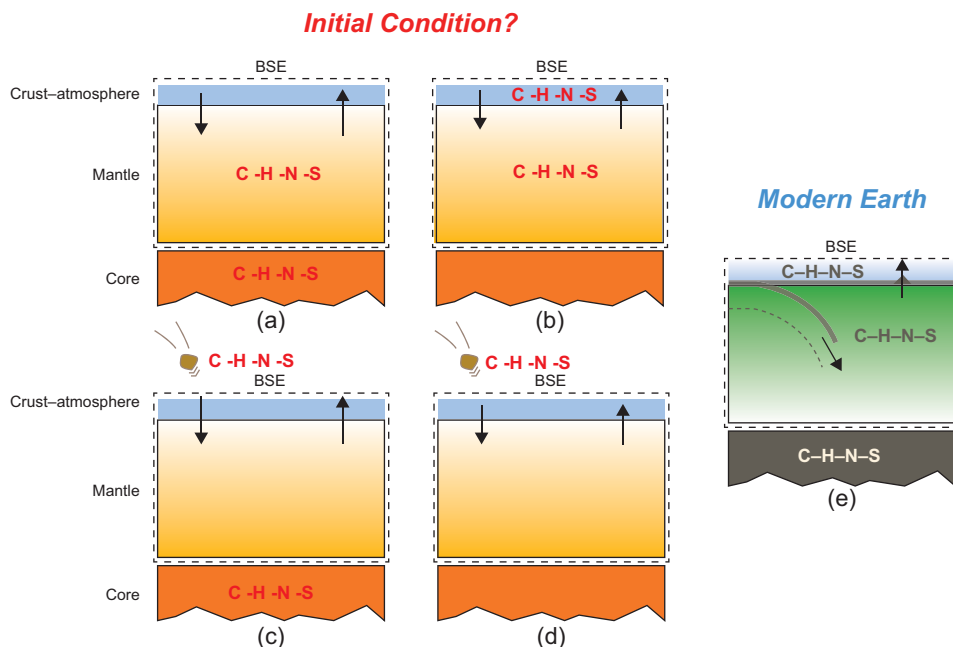


Figure 2.1 Plausible initial distributions of C, H, N, and S between Earth's major reservoirs at the end of accretion and core formation. (a) LEVEs are available during accretion and all LEVEs are initially sequestered in the core and the MO. (b) LEVE delivery during accretion is temporally separate from the main episodes of core formation and thus the core is effectively devoid of LEVEs. (c) Available LEVEs during accretion are effectively sequestered in the core or lost to space (not shown) and the BSE acquires LEVEs via later additions. (d) Core-mantle differentiation takes place in the absence of LEVEs and LEVEs are added via late additions. These distributions eventually evolved into the setup seen in the modern world (e), where these volatile elements are thought to exchange between Earth's mantle and the crust-ocean-atmosphere system (ingassing and outgassing) regulates the long-term habitability of the planet.

degassing, and atmospheric loss in shaping the absolute and relative abundances of C and the other LEVEs. The current understanding of the fractionation of C and other LEVEs during the core formation process will also be used to put constraints on the C budget of the core.

## 2.2 Constraints on the Compositions of Terrestrial Building Blocks

### 2.2.1 Constraints from Isotopes of Refractory Elements

Geochemical models based on elemental abundances and isotopic constraints predict the accretion of bulk Earth primarily from chondritic meteorites.<sup>25,26</sup> Because elemental and isotopic fractionation trends for bulk silicate samples and chondritic meteorites have well-defined relationships, it is widely assumed that the building blocks of Earth belong to a class of primitive objects that are sampled by chondritic meteorites.<sup>27</sup> Close similarity of the

abundances of refractory lithophile elements between the BSE and CI led to an early development of a CI model for Earth.<sup>25</sup> Allègre et al.<sup>27</sup> further consolidated this model by arguing that volatile depletion trends in the BSE are matched most closely by CI chondrites. However, a distinct disparity of oxygen (second most abundant element in the BSE by mass) isotopes (i.e.  $^{16}\text{O}$ ,  $^{17}\text{O}$ , and  $^{18}\text{O}$ ) between CI chondrites and the BSE, which could not be explained by any fractionation or differentiation models,<sup>28,29</sup> was one of the first observed isotopic variations that challenged the CI model for Earth. Over the past decades, isotopic dissimilarity between CI chondrites and the BSE has been extended from  $\Delta^{17}\text{O}$  (deviation from a reference mass-dependent fractionation line in a triple isotope of oxygen plot<sup>30</sup>) to several radiogenic as well as non-radiogenic isotopic anomalies for a wide suite of refractory elements with contrasting geochemical behaviors: lithophile elements ( $\epsilon^{48}\text{Ca}$  (Ref. 31),  $\epsilon^{50}\text{Ti}$ ,  $\mu^{142}\text{Nd}$ ), moderately siderophile elements ( $\epsilon^{54}\text{Cr}$ ,  $\epsilon^{64}\text{Ni}$ ,  $\epsilon^{92}\text{Mo}$ ), and highly siderophile elements (HSEs;  $\epsilon^{100}\text{Ru}$ ) (Refs. 32, 33 and references therein). Interestingly, the BSE isotopic compositions for all of these elements are almost indistinguishable from enstatite chondrites (E-chondrites). This has led to the development of an E-chondrite model for Earth.<sup>32,34,35</sup> Tracking the isotopic evolution of the growing BSE by taking into account the alloy–silicate partitioning behavior of several lithophile, moderately siderophile, and HSEs during core–mantle equilibration, Dauphas<sup>32</sup> proposed that half of the first 60% of accreted mass was composed of E-type chondrites, while the remaining 40% was all E-type chondritic materials. However, there are a few outstanding issues with an E-chondritic model for Earth, namely: (1) the Ca/Mg ratio of the BSE (0.118<sup>36</sup>) is distinctly higher than that of E-chondrites (0.080<sup>37</sup>), suggesting that the BSE has an enriched refractory elemental abundance relative to E-chondrites;<sup>38</sup> (2) E-chondrites have an Mg/Si ratio that is lower than that of the BSE sampled by upper-mantle rocks,<sup>39</sup> which can only be explained by either incorporation of Si into the core or via an unsampled lower mantle with a low Mg/Si ratio;<sup>40</sup> and (3)  $\delta^{30}\text{Si}_{\text{BSE}}$  is 0.3–0.4‰ higher than  $\delta^{30}\text{Si}$  of E-chondrites and aubrites.<sup>41</sup> Experimentally determined Si isotopic fractionation parameters<sup>42,43</sup> rule out the possibility of explaining the Si isotopic composition as well as the Mg/Si ratio of the BSE via incorporation of Si in the core if Earth was primarily accreted from E-chondrites.<sup>41</sup> Although there are studies that argue for a lower mantle or at least a portion of the lower mantle being richer in silica compared to Earth's upper mantle,<sup>40,44</sup> such findings are debated. To circumvent these issues, Dauphas et al.<sup>45</sup> proposed that the bulk Earth and the E-chondrites sample an isotopically similar reservoir with their subsequent chemical evolution offset by ensuing nebular fractionation and planetary differentiation processes. In summary, a large number of geochemical systematics point to the bulk Earth being made from E-chondrite-type materials, although questions on the major element and volatile element abundance mismatch remain.

### 2.2.2 Constraints from Isotopes of Highly Volatile Elements

In contrast to constraints from refractory elements, constraints from highly volatile elements (i.e. C, N and H (water)) paint a different picture on the potential sources of LEVEs.

Although ordinary chondrites (OCs), which sample S-type asteroids in the inner belt (2.1–2.8 AU), have similar amounts of bulk water as the BSE, the D/H ratio of the BSE is not similar to that of OCs,<sup>46</sup> but rather is strikingly similar to that of carbonaceous chondrites, especially CI chondrites,<sup>47</sup> which are representative of C-type asteroids (beyond 2.8 AU) (Figure 2.2a). Similarity of  $^{15}\text{N}/^{14}\text{N}$  between the BSE and CI chondrites also points toward a carbonaceous chondritic origin of volatiles on Earth (Figure 2.3b).<sup>13,48,49</sup>  $^{13}\text{C}/^{12}\text{C}$  of the BSE cannot distinguish between a chondritic or cometary origin of C (Figure 2.2b).<sup>50,51</sup> However, a clear distinction of the  $^{15}\text{N}/^{14}\text{N}$  ratio of the BSE from the corresponding cometary values would necessitate C delivery by CI chondrites as well, assuming all the major volatiles (i.e. C, N, and water) were sourced from a similar parent body.

Although thus far direct matching of the isotopes of C, H, and N of the BSE with undifferentiated meteorites has been the approach<sup>59</sup> to determining the source of the LEVEs on Earth, there is a growing realization that there may be fractionation of stable isotopes during early terrestrial differentiation, such as devolatilization, MO degassing, and core–mantle fractionation. Indeed, such fractionation processes may be able to reconcile some of the observed differences between the LEVE isotopic compositions of the BSE and the chondrites.<sup>60</sup> For example, carbon isotopic compositions of many CI chondritic materials are distinctly lighter ( $\delta^{13}\text{C}$ , approximately  $-15$  to  $-7\%$ )<sup>50</sup> than the average carbon isotope composition of Earth's mantle ( $\delta^{13}\text{C}$ , approximately  $-5\%$ )<sup>61,62</sup>. Similarly, the sulfur isotope composition of Earth's mantle has also been argued to be non-chondritic.<sup>63</sup> Graphite–Fe–carbide melt carbon isotope fractionation experiments<sup>64</sup> showed that  $^{12}\text{C}$  preferentially incorporates into the metallic phase, leaving a  $^{13}\text{C}$ -enriched signature in the graphite or diamond. If similar fractionation behavior applies between silicate MO and core-forming alloy liquid, then core formation could explain how Earth's mantle evolved to have a heavier carbon isotope value compared to the chondritic building blocks.

### 2.2.3 Constraints from Theoretical Modeling

Because isotopic compositions of refractory elements suggest bulk Earth to be composed of materials similar to E-chondrites while volatile elements favor their delivery via CI chondritic material, the timing of admixing of C-rich material into the accreting zone of Earth becomes key. Such admixing could have taken place either during the primary stage of Earth's growth or after the main phase of accretion. Similarly, delivery of C-bearing materials may have occurred via accretion of undifferentiated bodies similar to chondrites or via amalgamation of differentiated bodies with C abundances in relevant reservoirs of those bodies set by core–mantle differentiation and atmospheric losses.<sup>16–18</sup> Theoretical models have been used to simulate the early evolution of the Solar System by accounting for dynamics of planetary accretion along with geochemical, cosmochemical, and chronological relationships between accreting and resulting bodies.<sup>65,66</sup> Constrains from Hf/W chronometry predict that Mars-sized planetary embryos were formed from mostly E-type

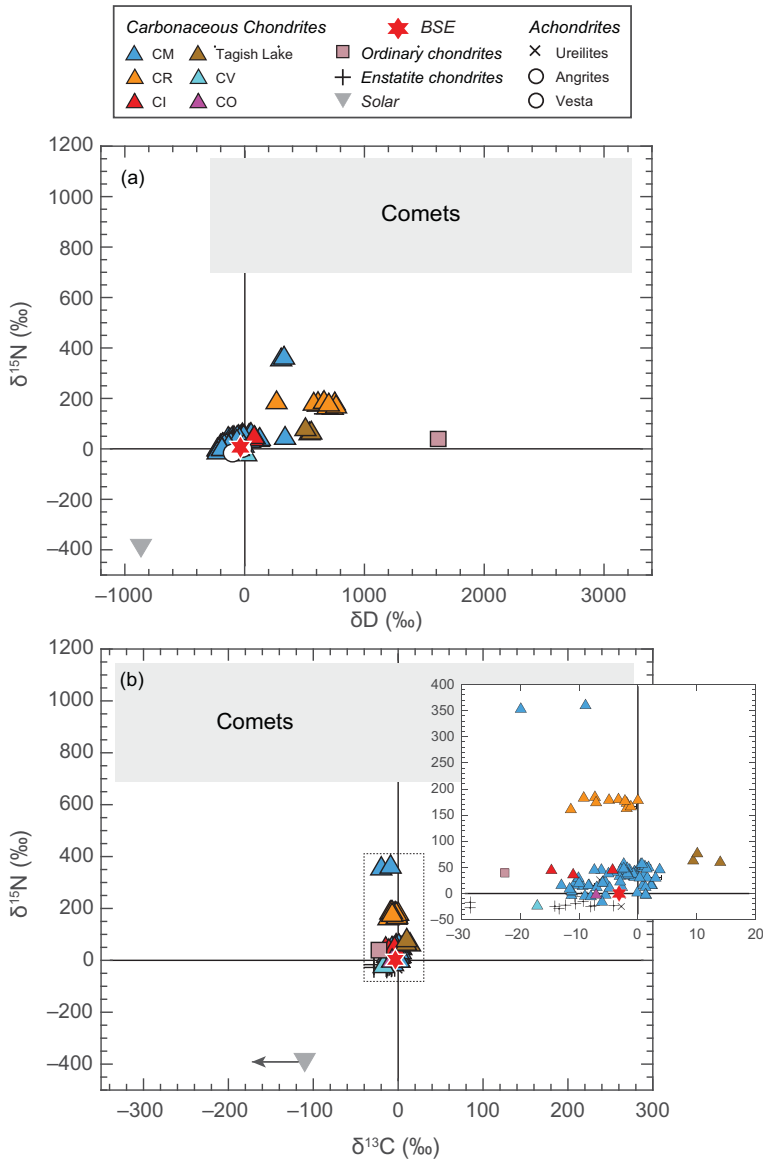


Figure 2.2 Comparison of isotopic compositions of (a) hydrogen and nitrogen and (b) carbon and nitrogen for several Solar System objects and reservoirs. The solar reservoir is depleted while the cometary reservoir is enriched in the heavier isotopes of nitrogen and hydrogen relative to all classes of meteorites as well as the BSE. Although  $\delta^{13}\text{C}$  alone cannot distinguish between the meteoritic and cometary sources, the isotopic compositions of all major LEVEs suggest that the BSE had a similar parent reservoir as carbonaceous chondrites.

Data sources: Carbonaceous chondrites, Refs. 48, 49; E-chondrites, Refs. 52, 53; comets, Ref. 54; angrites and Vesta, Refs. 51, 55; and solar, Refs. 56–58.

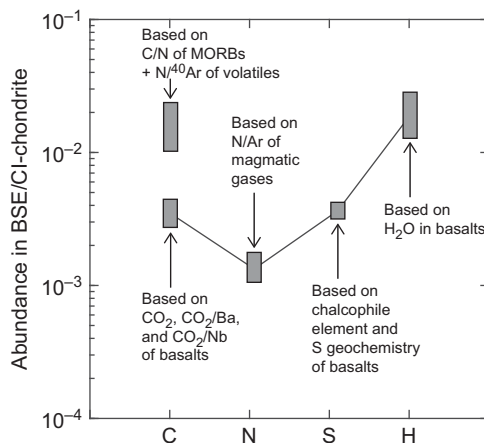


Figure 2.3 Comparison of the abundances of C, N, S, and H in the BSE normalized to their respective abundances in CI chondrites. In the BSE, C is enriched relative to N, has a similar abundance to S, and is depleted relative to H in comparison to its abundance in CI chondrites. Data from Refs. 10, 11, and 13. Also noted in the figure is the main geochemical information used to estimate the BSE concentrations of the respective elements in the original studies. MORB = mid-ocean ridge basalt.

chondritic material sourced from the inner part of the Solar System in the initial  $\sim 5$  Ma.<sup>67</sup> Recent advancements like pebble accretion models predict that gas giants like Jupiter also grew synchronously to their present-day mass via trapping of proto-solar nebular gas within the lifetime of the protoplanetary disk.<sup>68,69</sup> However, the growth of gas giants is thought to rapidly deplete the asteroid belt, which would mean minimal interaction of C-rich carbonaceous chondritic material that condensed in the outer parts of the Solar System with the growth zone of terrestrial planet accretion within 2 AU.<sup>19</sup> With the consideration that the presence of giant planets in the system affects the mixing and delivery of LEVEs from the outer regions to the terrestrial planet-forming region in the disk, the migration of giant planets has been argued to be necessary to perturb the orbits of cometary and asteroid-like bodies, bringing a fraction of these to the inner regions, where they can collide with terrestrial planets, delivering additional volatile elements to the rocky planets.<sup>19</sup> A specific planetary migration model, the Grand Tack scenario,<sup>19,20,65</sup> postulated that the inward and outward movement of Jupiter likely repopulated the asteroid belt in the inner parts of the Solar System with C-type chondritic material. However, these models cannot constrain the net mass of volatile-rich material being delivered, as they allow for a total influx of volatile-rich material  $\geq 0.5$ –2.0% of present-day Earth's mass, assuming volatile-rich CI chondrites have water in the range of 5–10 wt.%.<sup>19,20</sup> Delivery of a C budget that is larger than the present day in the BSE would require offsetting via later differentiation processes, while C delivery being restricted to the present-day budget of the BSE would have to be unaffected by later differentiation processes. A model such as Grand Tack does not directly constrain the relative timing of acquiring the C- and water-rich



chondritic materials in the terrestrial planet-forming regions with respect to specific giant impact events. However, with the Moon formation being a specific event, similarity or a lack thereof between C and other LEVE budgets and volatile isotope signatures of Earth and Moon may shed light on when LEVE-rich materials were brought in with respect to the Moon-forming event. Little is known about the C budget of the Moon or the lunar mantle;<sup>70,71</sup> however, if water and carbon were co-delivered, the appreciable water content of lunar glasses and melt inclusions<sup>72,73</sup> and the E-chondritic nature of late veneer<sup>32</sup> can only be reconciled if volatiles were delivered to the Earth–Moon system before<sup>74,75</sup> or during the Moon-forming impact.<sup>18</sup> However, if C and other LEVEs were delivered during the main stage of Earth's accretion, then differentiation processes like core–mantle separation, as well as the delivery mechanism of volatiles – either by smaller, undifferentiated planetesimals composed of primarily CI-chondritic material or via relatively large, differentiated planetary embryos heterogeneously composed of material sourced from both inner and outer parts of the Solar System – can provide additional information on the origin of LEVEs in the BSE.

### 2.3 C and Other Volatiles: Abundances, Ratios, and Forms in Various Classes of Meteorites and Comparison with the BSE

The present-day BSE is estimated to be depleted in C and other highly volatile elements relative to all classes of undifferentiated meteorites by at least an order of magnitude and by as much as two orders of magnitude compared to the more primitive carbonaceous chondrites (Table 2.1).<sup>13</sup> For example, carbonaceous chondrites are C rich,<sup>48,54,76</sup> while enstatite and OCs are relatively C poor.<sup>54,61</sup> Among various carbonaceous chondrites, CI chondrites are the most C rich,<sup>54,76–79</sup> and they are also richer in other LEVEs such as N (0.19–0.32 wt.%<sup>54,76,77</sup>) and H (1.55–2.02 wt.%<sup>54,77</sup>) compared to other types of carbonaceous chondrites such as CV, CO, CM, and CR (Table 2.1). Severe depletion of C in the BSE relative to CI chondrites can be explained either by accretion of extremely small quantities of CI chondrites as late additions or via accretion of larger quantities of CI chondrites, but subject to subsequent loss during accretion or differentiation. Such loss of C from carbonaceous building blocks may be expected given that primary carbon is present as soluble as well as insoluble organic molecules in carbonaceous chondrites, which are expected to be unstable at the high temperatures occurring during inner-Solar System processes. Similarly, the carbonates that are products of secondary alterations in carbonaceous chondrites are also expected to volatilize during delivery and accretion in the inner-Solar systems bodies. Even though E-chondrites may have C abundances that are not much greater than that in the BSE, such concentrations are more likely to survive the delivery to the inner-Solar System bodies given their presence in the form of more refractory graphite, diamonds, and carbides.<sup>80</sup> It remains unclear, however, in what form and abundance C was in E-chondrite parent bodies before thermal metamorphism. It cannot be ruled out that unprocessed E-chondritic protoliths were more C rich and may have even contained



Table 2.1 *C content and C/S, C/N, and C/H weight ratios of major terrestrial reservoirs and chondritic building blocks*

Reservoirs	C (wt.%)	C/S	C/N	C/H
<i>Terrestrial reservoirs</i>				
BSE	$0.011 \pm 0.002$	$0.49 \pm 0.14$	$40.00 \pm 8.00$	$1.13 \pm 0.20$
Mantle	$0.008 \pm 0.002$	$0.36 \pm 0.10$	$72.73 \pm 37.72$	$2.00 \pm 0.70$
Crust–ocean–atmosphere	$0.002 \pm 0.000$	$8.89 \pm 2.22$	$12.5 \pm 3.22$	$0.51 \pm 0.04$
Core	0.50 (?)	0.32 (?)	85.00 (?)	8.40 (?)
<i>Carbonaceous chondrites</i>				
CO	$0.63 \pm 0.24$	$0.32 \pm 0.12$	$21.74 \pm 19.16$	$10.40 \pm 0.00$
CV	$0.92 \pm 0.43$	$0.42 \pm 0.20$	$23.96 \pm 24.16$	$10.20 \pm 0.00$
CM	$1.89 \pm 0.48$	$0.58 \pm 0.15$	$21.01 \pm 8.35$	$3.20 \pm 0.00$
CI	$4.24 \pm 0.77$	$0.72 \pm 0.13$	$19.66 \pm 11.69$	$4.80 \pm 0.00$
<i>Enstatite chondrites</i>				
EH	$0.36 \pm 0.13$	$0.06 \pm 0.02$	$13.73 \pm 7.26$	$11.00 \pm 0.00$
EL	$0.48 \pm 0.16$	$0.15 \pm 0.05$	$24.43 \pm 9.40$	$11.00 \pm 0.00$
<i>Ordinary chondrites</i>				
H	0.11	0.06	$>104.00$	$2.50 \pm 0.70$
L	0.09	0.04	$46.10 \pm 1.00$	$3.00 \pm 1.00$
LL	0.09	0.05	$51.22 \pm 1.20$	$2.60 \pm 0.50$

The mantle, the crust-ocean-atmosphere, and the BSE averages and  $1\sigma$  standard deviations are from Hirschmann and Dasgupta<sup>7</sup> for C/H, Bergin et al.<sup>10</sup> for C/N, and Hirschmann<sup>11</sup> for C/S. The carbonaceous chondrite data for C, H, and N are from Figure 2.3, E-chondrite C/N data are from Grady et al.<sup>52</sup> and Alexander et al.<sup>53</sup> OC C/N data are from Bergin et al.<sup>10</sup> and references therein. The C/S data for all chondrites are from Wasson and Kallemeyn,<sup>37</sup> and the C/H data for enstatite and OCs are from Hirschmann<sup>11</sup> and references therein. The core compositional estimates are using bulk Earth concentrations from McDonough,<sup>83</sup> and  $D_{\text{alloy/silicate}}^x$  values are from Figure 2.5 and assuming complete core–mantle equilibration. The data for C contents are from Bergin et al.<sup>10</sup> for terrestrial reservoirs, from Alexander et al.<sup>48</sup> for carbonaceous chondrites, from Grady et al.<sup>52</sup> for E-chondrites, and from Wasson and Kallemeyn<sup>37</sup> for OCs.

organics. Despite the survival potential of refractory C-bearing phases in E-chondrites in the inner-Solar System processes, it is generally thought that the E-chondrites had much less water than the present-day BSE,<sup>81</sup> although the H budget of the BSE has significant uncertainty owing to poor constraints on the water budget of the mantle.<sup>82</sup>

In contrast to absolute abundances, the relative abundance of C with respect to other volatile elements in the BSE (i.e. C/H, C/N and C/S) is a powerful tracer to constrain the C abundance of Earth and provides additional constraints on the processes that must have fractionated the geochemical reservoirs relative to the cosmochemical reservoirs (Figure 2.3).

Due to the comparable 50% condensation temperatures of C and N as well as their abundances being positively correlated in various classes of chondrites, comparison of the

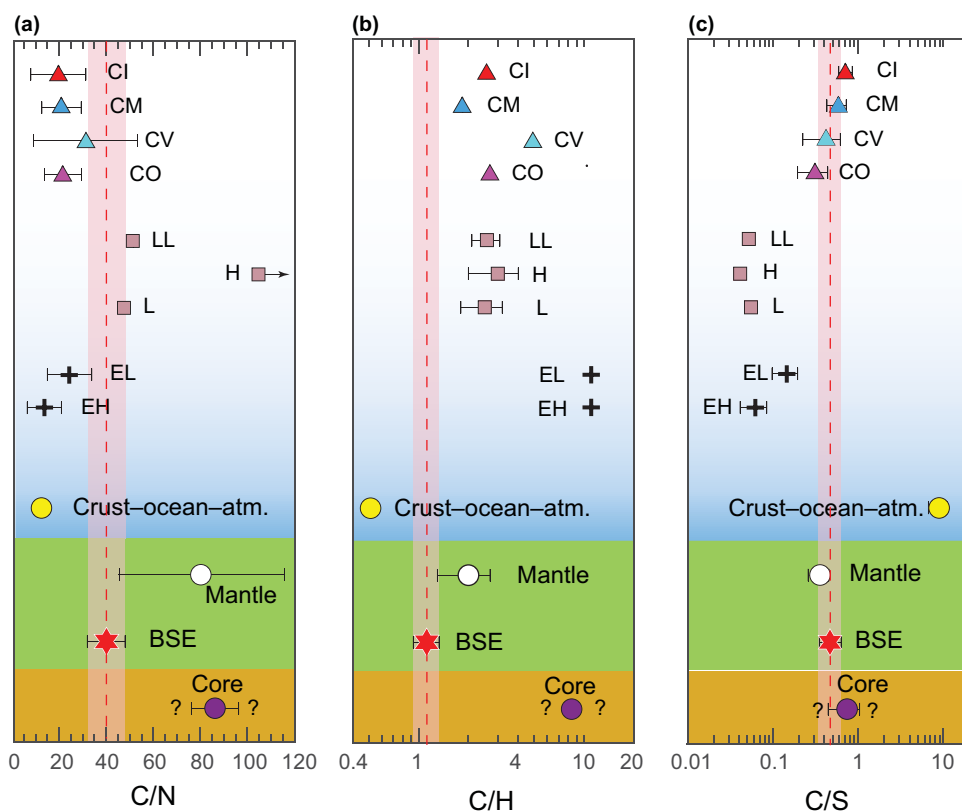


Figure 2.4 Comparison of bulk C/N (a), C/H (b), and C/S (c) weight ratios between different terrestrial and chondritic reservoirs. The data are from Table 2.1. CI = Ivuna-type Carbonaceous chondrite; CM = Mighei-type Carbonaceous chondrite; CV = Vigarano-type Carbonaceous chondrite; CO = Ornans-type Carbonaceous chondrite; LL = low total iron, low metal ordinary chondrite; H = highest total iron ordinary chondrite; L = low total iron ordinary chondrite; EL = (low enstatite) enstatite chondrite; EH = (high enstatite) enstatite chondrite.

C/N ratio of the BSE with that of the building blocks can help track the accretion and differentiation history of C in the early Earth. Recently, Bergin et al.<sup>10</sup> estimated the BSE C/N ratio to be  $40 \pm 8$  by calculating the mantle C content using  $\text{CO}_2/\text{Nb}$  and  $\text{CO}_2/\text{Ba}$  ratios of possibly undegassed ocean island basalts (Figure 2.3).<sup>84</sup> This C/N ratio is similar to the estimate of Halliday,<sup>12</sup> but lower than the estimate of Marty.<sup>13</sup> We will adopt the C/N ratio from the latest studies.<sup>11,18,85</sup> The C/N ratios of volatile-rich CI and CM as well as slightly volatile-poor CO and CV chondrites are lower than the C/N ratio of the BSE by approximately a factor 2, while E-chondrites also have low C/N ratios (5–25; Figure 2.4a). Although OCs show large scatter in C/N ratios due to uncertainties in determining extremely low C and N contents, their average C/N ratios are higher than that of the BSE (Figure 2.4a). Because the average C/N ratio of all classes of chondrites lies in the range of 5–30, the superchondritic

C/N ratio of the BSE has been postulated to be a legacy of either preferential incorporation of N into the core or loss of an early N-rich atmosphere.<sup>13</sup> However, ureilites, a class of achondrites and assumed to be the mantle restite of an asteroidal body, are extremely C rich (average 3 wt.% C) with intergranular veins of graphite and traces of diamonds.<sup>86,87</sup> It is interesting to note that the C/N ratio of ureilites is much higher than that of the BSE;<sup>11,88</sup> therefore, if the C/N ratios of this achondrite are representative of an ureilite parent body and such a parent body significantly contributed to Earth's accretion,<sup>89</sup> then preferential loss of N as a necessary condition for bulk silicate reservoirs in Earth is precluded.

Assuming a similar C inventory in the mantle as discussed earlier, the C/H ratio of the BSE has been estimated to be  $1.13 \pm 0.20$ .<sup>7,11</sup> The C/H ratio of BSE is lower than all classes of chondritic meteorites (Figure 2.4). OCs have a C/H ratio that is two to five times greater than that of the BSE, while E-chondrites, which are extremely water poor, have a 20-times higher C/H ratio. Carbonaceous chondrites, which have the closest match to the terrestrial D/H ratio, also have a higher C/H ratio; CI and CM chondrites, which are C and water rich, have a C/H ratio that is four to six times higher; while CO and CV chondrites, which are relatively C and water poor, have a C/H ratio that is 12–15 times higher. Therefore, in contrast to a superchondritic C/N ratio, a subchondritic C/H ratio can be explained if C was preferentially incorporated into the core or lost to space relative to H during terrestrial differentiation.

Sulfur has a much higher solar nebula condensation temperature than C, N, and H; therefore, it is not a highly volatile element. Sulfur abundance in the BSE, especially in the mantle, is also better known<sup>90–92</sup> relative to that of other highly volatile elements of interest (Figure 2.3). Therefore, the C/S ratio can also act as an important tracer to track the evolution of C in the early Earth. The C/S ratio of the BSE is higher than that of C-depleted E-chondrites, but it is similar to or lower than that of C-rich carbonaceous chondrites (Figure 2.4c). Therefore, a near-chondritic C/S ratio in the BSE stipulates that either both C and S showed similar loss/gain behavior during early differentiation processes or they were primarily delivered in post-differentiation processes via undifferentiated, chondritic materials.

Because the C/H ratio of the BSE is subchondritic, the C/S ratio is near-chondritic, while the C/N ratio is superchondritic, H, N, and S have widely different geochemical behaviors relative to C during core formation or MO degassing and/or they track different stages of terrestrial accretion. The following sections will explore whether there are known processes that can explain the difference between the LEVE geochemistry of the BSE and those of carbonaceous chondrites.

## 2.4 Establishing LEVE Budgets of the BSE After Core Formation?

### 2.4.1 The Role of Late Accretion

The theory of the addition of undifferentiated meteorites after the completion of metal–silicate differentiation chiefly stems from the approximately chondritic relative abundance of HSE (e.g. Re, Os, Ir, Ru, Pt, Rh, Pd, and Au) concentrations in Earth's mantle and the

BSE, plus the fact that the BSE is not as depleted of HSEs as it would have been if the entire HSE inventory of the bulk Earth was available before equilibrium core formation took place.<sup>93,94</sup> Assuming that core formation originally left the silicate Earth virtually HSE free and later additions of chondritic materials elevated the HSE abundances to the present level, the chondritic mass added is estimated to be 0.5% of Earth's mass ( $0.005 M_E$ ). Walker<sup>93</sup> noted that this estimate may be ~1.5 times higher or a factor of four lower<sup>95</sup> depending on the exact concentrations of HSEs in the chondritic materials being added. Willbold et al.<sup>96</sup> also calculated that in order to offset the pre-late accretion <sup>182</sup>W-excess composition of the BSE,  $0.08 M_E$  chondritic mass needs to be added. Given that many carbonaceous chondrites are rich in LEVEs, many studies have surmised that late accretion of these materials brought all of the LEVEs to the BSE.<sup>71,97–99</sup> If this was the mechanism, then the core formation would have no influence on the relative abundance of various LEVEs. Indeed, the addition of  $0.0030–0.0075 M_E$  chondritic materials with 3.48–3.65 wt.% C to the BSE would set the BSE C budget to ~100–250 ppm C (or ~360–900 ppm CO<sub>2</sub> in the mantle<sup>8</sup>). Although this C budget may be sufficient to match even the enriched basalt source regions, as briefly discussed by Dasgupta,<sup>8</sup> there are several challenges in invoking CI-type carbonaceous chondrite as the chief or sole source of the BSE C and other LEVEs. Section 2.2 already discussed which elemental and isotopic compositions of the BSE are not satisfied if the BSE is chiefly made up of carbonaceous chondrites. Section 2.2 also outlined how the elemental abundance of C and the C/S ratio of the BSE can be satisfied if CI-type carbonaceous chondrite accreted to Earth after core formation was complete, but the C/N and C/H ratios and possibly  $\delta^{13}\text{C}$  and  $\delta^{34}\text{S}$  of the BSE are difficult to explain. Here, we specifically discuss what challenges exist in invoking other known meteorites as the late-accreting materials to explain the entire inventory of carbon and other LEVEs in the BSE.

Given E-chondrites (e.g. (low enstatite) enstatite chondrite (EL) and (high enstatite) enstatite chondrite (EH)) are depleted in water and also poor in C and N,<sup>52</sup> bringing LEVEs in general and water in particular to Earth exclusively by E-chondrite is not thought to be a realistic mechanism. EH and EL chondrites also have distinctly lower C/N and C/S ratios compared to the BSE (Figure 2.4a and c). Hence, unprocessed E-chondrite, known from the studied samples, could not have brought LEVEs to Earth after core formation in the right proportions. This is at odds with recent propositions that, based on Ru isotopic composition, argued for the late veneers having E-chondritic character.<sup>32,33</sup> One issue in evaluating E-chondrites as plausible terrestrial building blocks based on volatile element geochemistry is that all known E-chondrites studied thus far are heavily metamorphosed; hence, before thermal metamorphism, these chondrites might have been more LEVE rich and C could have been originally organic.<sup>100</sup>

OCs are depleted in volatiles with respect to carbonaceous chondrites chiefly because the volatile-rich matrix volume percentage is less than that of carbonaceous chondrites.<sup>54</sup> In fact, bulk C content of most primitive OCs can be perfectly explained by its matrix material being entirely CI-type material.<sup>48</sup> OC matrices are drier, however, with bulk H of

OCs falling below the concentration of what would be expected if the entire OC matrix was made up of CI-type materials.<sup>54</sup> Therefore, the C/H ratio of OCs is higher than that of the BSE (Figure 2.4b). Similarly, the C/S ratios of OCs are lower and the C/N ratios of OCs are distinctly higher compared to the estimates for the BSE (Figure 2.4a and c). Hence after core formation, OC delivery cannot be considered as the chief process of origin of Earth's LEVEs.

Among all stony meteorites, ureilites are the only group of primitive achondrites that are rich in C and depleted in N, leading to higher C/N ratios.<sup>101–103</sup> Carbon in ureilites is also present in relatively non-labile phases (i.e. as graphites, nanodiamonds, and lonsdaleite) and hence is likely to survive high-temperature accretional processes. Primarily motivated by their high C/N ratios, recent studies<sup>11,88</sup> have suggested that C-rich achondrites such as ureilites may be responsible for establishing the abundances of LEVEs in the BSE through post-core formation addition. While the C/N ratio of the BSE could be heavily shaped by the addition of a ureilite-like achondrite, the C/S ratio of ureilite is significantly higher than that estimated for the BSE. Hence, any attempt to match the C/S ratios of the BSE through addition of a ureilite-like achondrite-rich late veneer requires a very unique consideration of the composition and extent of core–mantle equilibration of proto-Earth.<sup>11</sup> No model of ureilite-like late-veneer addition can explain the C/N and C/S ratios simultaneously. For example, scenarios of C-rich late-silicate addition in which the superchondritic C/N ratio can be established also result in a superchondritic C/S ratio.<sup>11</sup>

Overall, late accretion alone does not seem to account for the C budget and C to other LEVE ratios of the present-day BSE (Figure 2.5). Hence, other early Earth processes need to be considered.

#### 2.4.2 The Role of Post-core Formation Sulfide Segregation

The segregation of sulfide melt has been shown to be a necessary process for explaining the HSE geochemistry of the BSE.<sup>112</sup> This would also deplete the BSE in terms of its S inventory, but owing to the low solubility of C in sulfide-rich melts (Figure 2.6a)<sup>17,18,113–116</sup> caused by strong non-ideality of mixing between C- and S-rich components in Fe-rich alloy melts, such sulfide segregation should also elevate the C/S ratio of the BSE. Hence, if late accretion establishes a chondritic C/S ratio, sulfide segregation should alter such a ratio. N also is not compatible in S-rich Fe-alloy melts,<sup>18</sup> hence the S/N ratio of the BSE would also drop after sulfide melt segregation. Similarly, it is also unclear what the effects of late-stage sulfide melt segregation might be on the H budget of the BSE. If H is stored in nominally anhydrous silicate minerals in solid, post-core formation BSE, partitioning of H between segregating sulfide melts and solid silicate minerals could influence the H inventory and hence the C/H ratio of the BSE. If H partitions preferentially into sulfide liquid over relevant nominally anhydrous silicate minerals, then the C/H ratio may also increase above the chondritic value.

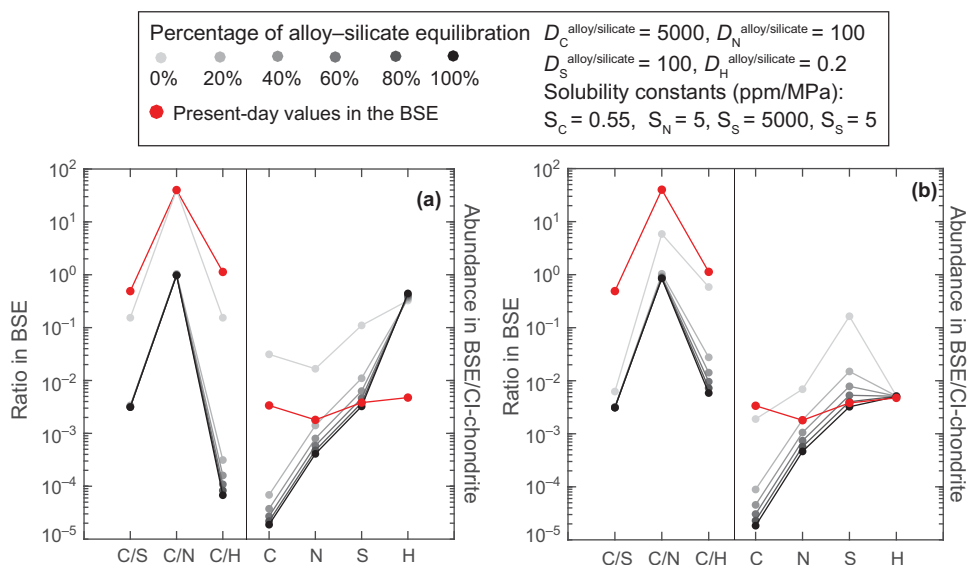


Figure 2.5 Application of alloy-silicate partition coefficients and solubilities of LEVEs in the silicate melts to examine the effect of core formation, with varying degrees of alloy-silicate equilibration, with or without loss of an early atmosphere formed via MO degassing on the remnant abundances of LEVEs in the bulk silicate reservoir. (a) LEVEs, when delivered as 0.015  $M_{\text{E}}$  late-accreting materials (i.e. 0% alloy-silicate equilibration), cause the volatile abundance to be higher than the present-day BSE. Core formation with increasing degrees of alloy-silicate equilibration increasingly depletes the remnant MO in all LEVEs, with C being much more depleted than other LEVEs, leading to subchondritic C/N, C/H, and C/S ratios. (b) Combining early atmospheric loss with core formation cannot offset C loss to the core due to the lower solubility of C relative to the other LEVEs in the silicate MOs. Bulk Earth volatile abundance data are from McDonough,<sup>83</sup> while the alloy-silicate partition coefficients in a deep MO ( $P = 50$  GPa,  $T = 3500$  K; e.g. Siebert et al.<sup>104</sup>) for C, N, S, and H are from the parametrized relationships of Chi et al.,<sup>71</sup> Grewal et al.,<sup>105</sup> Boujibar et al.,<sup>106</sup> and Clesi et al.,<sup>107</sup> respectively. Solubility constant data for C, N, S, and H in the silicate melt are from Armstrong et al.,<sup>108</sup> Roskosz et al.,<sup>109</sup> O'Neill and Mavrogenes,<sup>110</sup> and Hirschmann et al.<sup>111</sup>

### 2.4.3 The Role of MO-Atmosphere Interactions and Atmospheric Loss

Because C and other LEVEs are atmophile elements, they were likely heavily concentrated in the proto-atmospheres at various stages of MO evolution and terrestrial accretion. Hence, it is worth considering under what circumstances silicate magma-atmosphere interactions and possible atmospheric loss through impact-driven blow-off<sup>23</sup> could influence the inventory of LEVEs in the BSE. The timing of LEVE delivery is of critical importance in determining the role of silicate-atmosphere interactions (and atmospheric blow-off). For example, if a large fraction of core formation takes place before the LEVEs were available to the growing Earth,<sup>20,118</sup> then such core formation would have had negligible influence on the BSE LEVE budget, with MO-atmosphere processes being more important. On the other hand, if LEVEs were delivered throughout the terrestrial

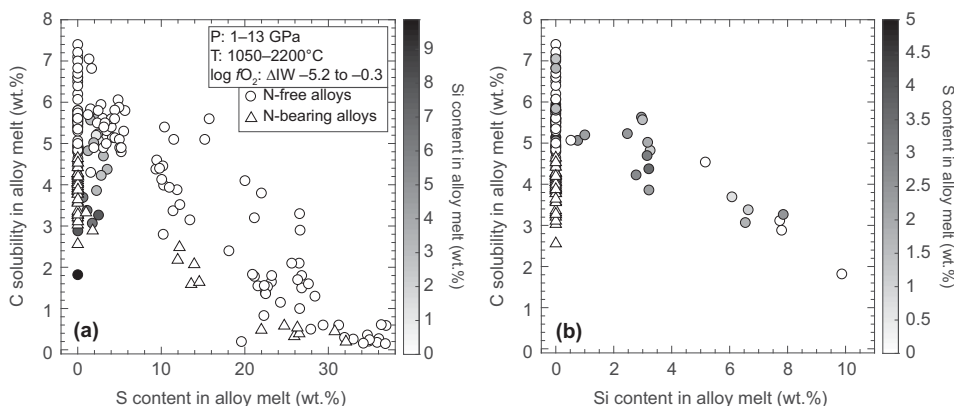


Figure 2.6 Experimental data showing the effects of S and Si contents in the Fe-rich alloy melt on C solubility. (a) Carbon solubility decreases monotonically with increases in sulfur content in the alloy melt. Si- and N-bearing alloys have lower C solubility for a given S content in the alloy melt. (b) Carbon solubility decreases linearly with increases in Si content in the alloy or decreases in oxygen fugacity ( $f_{\text{O}_2}$ ) of silicate–alloy systems. The presence of S in the alloy does not have a major effect on carbon solubility in silicon-bearing alloys.

Data for N-free alloys are from Dasgupta et al.,<sup>99,114</sup> Chi et al.,<sup>71</sup> Armstrong et al.,<sup>108</sup> and Li et al.,<sup>16,117</sup> while data for N-bearing alloys are from Dalou et al.<sup>85</sup> and Grewal et al.<sup>18</sup>

accretion history,<sup>13,51,119</sup> then both atmosphere–MO interactions and metal–silicate equilibration could have played roles in establishing the LEVE budget of the BSE.

If the BSE C–N–S–H budgets were established chiefly by loss of proto-atmosphere overlying MO, then N needed to be lost preferentially to C and C needed to be lost preferentially to H. In other words, the proto-atmosphere overlying MO has to be N rich relative to C, C rich relative to H, and with similar abundances of C and S. Indeed, the N-depleted nature of Earth has been explained previously by loss of an N-rich atmosphere.<sup>120</sup> But evaluation of whether an atmosphere with a concentration of LEVEs in the order  $\text{N} > \text{C} \sim \text{S} > \text{H}$  can be generated overlying a silicate magma reservoir depends on the mixed-volatile solubility in shallow MO as a function of oxygen fugacity ( $f_{\text{O}_2}$ ; effective partial pressure of oxygen). Hirschmann<sup>11</sup> considered a simple model evaluating the fractionation of C, N, H, and S between silicate MO, overlying atmosphere, and equilibrating core-forming liquid alloy with three distinct  $f_{\text{O}_2}$  conditions at the MO surface (i.e.  $\text{IW} - 3.5$  (reduced),  $\text{IW} - 2$  (intermediate  $f_{\text{O}_2}$ ), and  $\text{IW} + 1$  (oxidized), where IW refers to the  $\log f_{\text{O}_2}$  set by equilibrium of metallic iron and iron oxide ( $\text{FeO}$ )). Among these, the most oxidizing condition is not very realistic during or soon after core formation because, for a well-mixed MO with a near-constant  $\text{Fe}^{3+}/\text{Fe}_\text{T}$  ratio, the  $f_{\text{O}_2}$  gradient is such that the shallow MO is always more reduced.<sup>121–123</sup> Thus, if a well-mixed MO is close to equilibrium with an Fe-rich core at its base, its surface should be more reduced and therefore, for MO–atmosphere interactions, the relevant  $f_{\text{O}_2}$  would be less than IW. The only way this



may be different is if at higher pressures the  $f\text{O}_2$  gradient reverses (reduction with increasing depth) and iron disproportionation and subsequent Fe–metal segregation leads to oxidation of metal-free MO.<sup>124</sup> Solubility data for most LEVEs are lacking or sparse for peridotitic or ultramafic silicate melts due to difficulty in obtaining a glass and reliable chemical analyses for such compositions.<sup>125</sup> Based on the data available for silicic to mafic silicate liquids, for  $\log f\text{O}_2 < \text{IW} - 0.5$  and with decreasing  $f\text{O}_2$ , N becomes much more soluble (reaching the weight percentage level chiefly as N–H species<sup>85,126,127</sup>) than C (tens of ppm by weight mostly as  $\text{CO}_3^{2-}$  and to some extent as C–H and C–N species<sup>18,71,99,108,117,125,128,129</sup>), with the latter mostly decreasing with decreasing  $f\text{O}_2$  and then leveling off with stabilization of C–H species. Similar to N, H also remains quite soluble in silicate melt in the form of  $\text{OH}^-$  and  $\text{H}_2\text{O}$  even in fairly reducing conditions such as  $\log f\text{O}_2$  of  $\text{IW} - 1$  to  $\text{IW} - 2$ , with molecular hydrogen,  $\text{H}_2$ , contributing to some degree.<sup>111</sup> Therefore, at  $\log f\text{O}_2 < \text{IW} - 1.5$ , atmospheric blow-off could lower the C/H ratio from a chondritic value, but this would result in an MO C/N ratio that is subchondritic. Similarly, S is much more soluble in mafic–ultramafic silicate melts (several thousands of ppm<sup>110,130,131</sup>) compared to C and hence loss of an atmosphere would result in a residual silicate MO with a C/S ratio distinctly lower than that of chondritic value. Therefore, no condition exists where a proto-atmosphere overlying an MO can attain all of the compositional characteristics necessary to leave an MO with C/N, C/S, and C/H ratios of the modern-day BSE (Figure 2.5). Hence, late accretion of chondritic materials to an alloy-free MO followed by an atmospheric loss cannot be the chief origin of BSE LEVEs.

An alternative suggestion<sup>120</sup> is for atmospheric loss to help define the BSE C/N and C/H ratios, but at conditions where C would be retained in the form of carbonate or bicarbonate ions either as dissolved aqueous species or in the crust, mediated by the presence of a liquid water ocean. According to this model, a superchondritic C/N ratio and a subchondritic C/H ratio could have been attained via loss of an N-rich atmosphere overlying an ocean. This mode of atmospheric loss is supported by the dynamical model of a giant impact that shows that such an impact would preferentially remove the atmosphere relative to the ocean.<sup>132</sup> However, it is unclear what the water chemistry would be in these oceans, which, if they existed, is expected to be highly anoxic and thus may not sequester significant dissolved carbonates.

## 2.5 Establishing the Volatile Budget of the BSE through Equilibrium Accretion and MO Differentiation

The discussion on the origin of LEVEs in the BSE thus far considered building blocks and processes after the core formation was mostly complete. This approach would be appropriate if all of the LEVEs were delivered through late accretions. The discovery of a solar component (e.g. neon) in deep plume-derived magma,<sup>133,134</sup> however, suggests that Earth might have trapped nebular gas early within the first few millions of years of the formation

of the Solar System. Indeed, the possibility of acquiring volatile elements such as primordial noble gases directly from nebular gas has been proposed in a number of studies.<sup>135,136</sup> Although nebular gas can persist for  $\sim 10$  Myr, its median lifetime (i.e. the time at which half of all systems lost their nebular gas disks) is  $\sim 2.5$  Myr.<sup>137</sup> Given the mean time of terrestrial accretion (i.e. the time to have grown to 50% of the final mass) is  $\sim 11$  Myr<sup>138</sup> while the mean accretion timescale of Mars is  $1.9^{+1.7}_{-0.8}$  Myr,<sup>67,139</sup> it is likely that although the entire proto-Earth mass may not have equilibrated with the solar nebula, at least a few Mars-sized embryos that contributed to the initial proto-Earth mass likely inherited nebular volatiles. These constraints suggest that early accreting material may have been LEVE poor but likely not LEVE free. However, the LEVE compositions do not suggest direct Solar contribution to be important (Figure 2.2).

The  $^{182}\text{Hf}/^{182}\text{W}$  ratio of iron meteorites suggests metal–silicate separation in protoplanetary bodies occurred as early as  $\sim 1$  Myr after the formation of the Solar System. Accordingly, core formation would influence the initial distribution of LEVEs among the planetary reservoirs.<sup>8,11,14,16,17,71,85,99,117</sup> Over the past decade, a significant body of research has tried to understand the fate of C and other LEVEs (S, N, and H) during core formation processes and associated alloy–silicate equilibration.<sup>14–18,71,85,99,106,109,117,140–142</sup> These investigations chiefly focused on determining the partition coefficients of LEVEs between Fe-rich alloy melts and coexisting silicate melts (i.e.  $D_x^{\text{alloy/silicate}}$  (= concentration of an element in the alloy melt divided by concentration of the same element in the equilibrium silicate melt), where  $x = \text{C, N, S, etc.}$ ). If  $D_x^{\text{alloy/silicate}} > 1$  and if a given LEVE,  $x$ , is available during core formation, then it should be preferentially sequestered in the metallic core. On the other hand, if  $D_x^{\text{alloy/silicate}} < 1$ , the LEVE,  $x$ , present during core–mantle fractionation should preferentially concentrate in the silicate Earth.  $D_x^{\text{alloy/silicate}}$  values provide the framework to understand how a given LEVE is expected to be distributed between the metallic and silicate portions of a differentiated planet if alloy and silicate melts equilibrated before separation.

The most robust constraints available on the alloy–silicate partitioning of LEVEs are obtained through high pressure–temperature experiments. Determinations of  $D_C^{\text{alloy/silicate}}$  at high pressure–temperature exist chiefly for graphite/diamond-saturated conditions (i.e. experiments conducted in graphite capsules). Concentrations of C in Fe-rich alloy melts at graphite/diamond saturation and in the absence of any other light nonmetals show small dependence on pressure and temperature (not shown)<sup>14,16</sup> and are  $\sim 5\text{--}7$  wt.%. However, C solubility in Fe-rich alloy melts decreases strongly with increasing S and Si content, and at S of content 22–36 wt.% or Si content  $> 10\text{--}12$  wt.%, C solubility is  $< 1$  wt.% (Figure 2.6a and b). Carbon solubility in Fe-rich alloy melts also diminishes with increasing Ni content in the S-free or S-poor alloy.<sup>71,115,116,143</sup> Unlike in alloy melts, C solubility in equilibrium silicate melts is tens to hundreds of ppm and mostly decreases with decreasing  $f\text{O}_2$  (Figure 2.7). The MOs of Earth and other inner-Solar System bodies are expected to be ultramafic to mafic; that is, relatively poor in silica and rich in MgO.

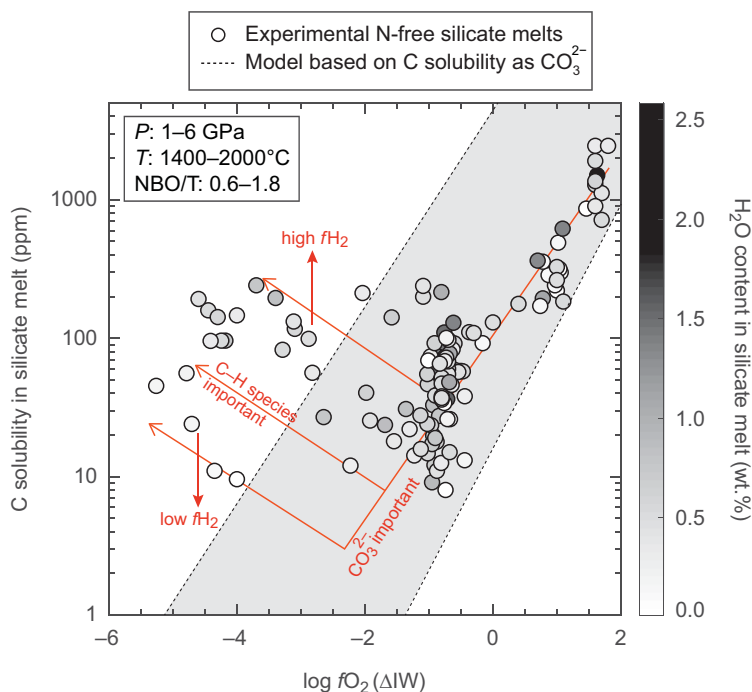


Figure 2.7 Experimental data showing the effects of  $fO_2$  and water content in the silicate melt on C solubility. Carbon solubility decreases with decreasing  $\log fO_2$  until  $\sim \Delta IW$  of  $-2$  to  $-1$  followed by an increase below  $\sim \Delta IW - 2$  depending upon bulk water content in the silicate melt. This change is likely caused by the change in contributions of C as  $CO_3^{2-}$  at higher  $fO_2$  and C as C–H species such as methyl groups at lower  $fO_2$ . The pressure–temperature–composition (expressed as NBO/T) condition of the experimental glasses are given in the legend. The shaded region represents predicted solubility of C as  $CO_3^{2-}$  at graphite saturation based on the model of Eguchi and Dasgupta<sup>146</sup> for the entire pressure, temperature, and  $X_{H_2O}$  space of the experimental data, while the NBO/T parameter is extrapolated for peridotite-like silicate melts (NBO/T = 2.7).

Data for N-free silicate melts are from Refs. 16, 17, 71, 99, 108, 117, 125, 129, 152, and 157.

Because of the difficulty of rapidly cooling such depolymerized silicate liquids from well-constrained high pressures–temperatures to glasses at ambient conditions, which is necessary for reliable quantitative analyses of carbon and hydrogen, C solubility data in such ultramafic–mafic liquids at core-forming reduced conditions are sparse.<sup>125</sup> To address this, experimental studies have been conducted with a silicate melt of varying polymerization so that a meaningful extrapolation of C solubility and  $D_C^{\text{alloy/silicate}}$  to desired silicate melt composition can be made.

### 2.5.1 Carbon Speciation in MO

$D_C^{\text{alloy/silicate}}$  and C solubility in silicate melts are affected by the incorporation mechanism of C in the silicate melt structure. Irrespective of the saturating phase such as  $\text{CO}_2$ -bearing vapor or graphite/diamond, carbon can dissolve in silicate melt as molecular  $\text{CO}_2$  ( $\text{CO}_2^{\text{mol}}$ , 144–148), as carbonate anions ( $\text{CO}_3^{2-}$ , 125, 149, 150) bonded to cation modifiers, possibly as molecular CO or carbonyl, 151, 152 and as possible C–H, C–N complexes. 18, 117 For mafic–ultramafic melts, the chief species of interest is  $\text{CO}_3^{2-}$ , which complexes most strongly with  $\text{Ca}^{2+}$  cations and also with  $\text{Na}^+$ ,  $\text{Mg}^{2+}$ , and maybe  $\text{K}^+$ . 125, 146, 153–156 Most experiments on carbon dissolution at reducing conditions employed mafic compositions of variable degrees of polymerization (i.e. tholeiitic to alkali basalts or even more silicic melts). The most common approach to extrapolating C solubility and  $D_C^{\text{alloy/silicate}}$  to systems containing peridotitic compositions is to use a compositional parameter NBO/T, where “NBO” is the total concentration of non-bridging oxygen in the silicate melt and “T” is the total number of tetrahedral cations. Although this method is thought to give reasonable predictions of ultramafic melt C solubility as  $\text{CO}_3^{2-}$ , Duncan et al. 125 showed that the NBO/T approach may overpredict the extent of  $\text{CO}_3^{2-}$  dissolution in silicate melts if an increase of NBO/T is correlated with an increase in CaO rather than MgO in melts. This is because  $\text{Ca}^{2+}$  cations complex with  $\text{CO}_3^{2-}$  much more than  $\text{Mg}^{2+}$ , 146 although peridotitic melts are still predicted to have higher  $\text{CO}_3^{2-}$  dissolution capacities than basalts. Figure 2.7 shows  $\text{CO}_3^{2-}$  dissolution as a function of  $f\text{O}_2$  and shallow MO conditions. Also shown in Figure 2.7 are other possible species such as C–H that may become important at low  $f\text{O}_2$ .

### 2.5.2 $D_C^{\text{alloy/silicate}}$ and Its Impact on Carbon Distribution between BSE versus Core in Various Scenarios of Equilibrium Core Formation

Figure 2.8 provides the available data of  $D_C^{\text{alloy/silicate}}$ , showing their dependence on alloy composition and  $f\text{O}_2$  at shallow MO conditions. Shallow MO  $D_C^{\text{alloy/silicate}}$  at  $\log f\text{O}_2$  of IW – 2 to IW – 0.5 are in the order of  $\sim 10^3$ , with the values increasing with increasing pressure and decreasing  $f\text{O}_2$  and decreasing with increasing temperature and melt depolymerization. 16, 71, 117 In more reducing conditions where the Si content becomes significant in the equilibrium Fe-rich alloy melts and where decreasing C dissolution as  $\text{CO}_3^{2-}$  is offset to some extent by the increasing fraction of C–H complexes (Figure 2.7),  $D_C^{\text{alloy/silicate}}$  may be somewhat lower and may not monotonically increase with decreasing  $f\text{O}_2$  (Figure 2.8b). 16, 117 Application of empirical parameterizations of  $D_C^{\text{alloy/silicate}}$  as a function of temperature, pressure,  $f\text{O}_2$ , silicate melt composition, and alloy composition (e.g. Ni content) to conditions that many studies considered relevant for the deep terrestrial MO (e.g. pressure = 45–65 GPa, temperature = 3500–4000 K,  $\log f\text{O}_2 = \text{IW} - 2$ ) yields values in the order of  $10^3$ – $10^4$ . The existing constraints on  $D_C^{\text{alloy/silicate}}$  in graphite-saturated conditions therefore suggest that carbon is highly siderophile. If core formation was an equilibrium process (i.e. if the entire terrestrial core mass equilibrated with a global silicate MO), post-core formation silicate Earth would be severely depleted in carbon ( $\ll 10$  ppm),

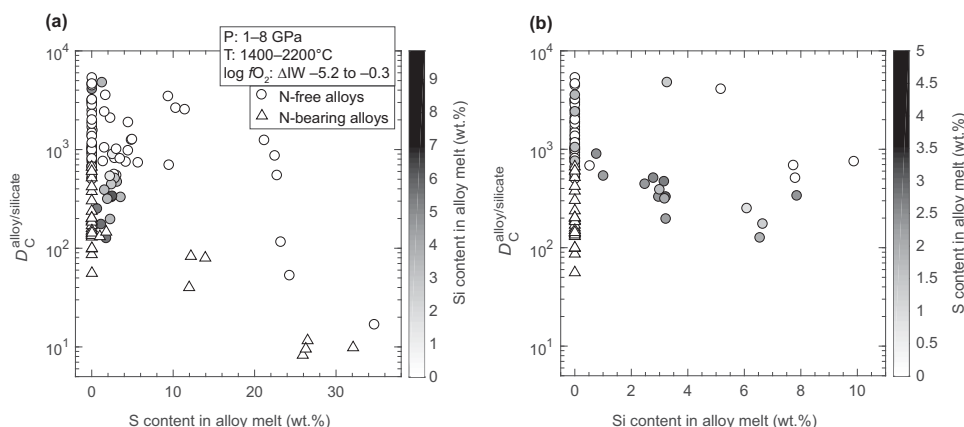


Figure 2.8 Experimental data showing the effects of S and Si in Fe-rich alloy melts on  $D_C^{\text{alloy/silicate}}$ . (a)  $D_C^{\text{alloy/silicate}}$  decreases with increases in S content in the alloy melt. (b)  $D_C^{\text{alloy/silicate}}$  decreases with increases in Si content in the alloy or indirect decreases in  $fO_2$  of the alloy–silicate systems. The presence of S in Si-bearing alloy melts generally decreases  $D_C^{\text{alloy/silicate}}$  in comparison to S-free systems.

Data for N-free alloys are from Dasgupta et al.,<sup>99,114</sup> Chi et al.,<sup>71</sup> Armstrong et al.,<sup>108</sup> Li et al.,<sup>16,117</sup> and Tsuno et al.,<sup>17</sup> while data for N-bearing alloys are from Dalou et al.<sup>85</sup> and Grewal et al.<sup>18</sup>

with the extent of depletion being dependent upon the available bulk carbon that participates in such core–mantle fractionation.<sup>8,17,71,99</sup> This analysis does not imply that the core formation process was a single-stage alloy–silicate equilibration event, but rather what the C distribution between Earth’s metallic and nonmetallic portions would be for an average condition of core–mantle separation.

Figure 2.9 shows more realistic scenarios of alloy–silicate equilibration and subsequent core segregation in terrestrial MO where the depth, temperature, and  $fO_2$  evolve with the extent of accretion.<sup>158</sup> This style of core–mantle fractionation is described as multistage, equilibrium core formation. Competing arguments exist in the literature as to whether, with continuing accretion, proto-Earth’s MO evolved from a relatively reduced to an oxidized condition<sup>158,159</sup> or a relatively oxidized to a reducing condition.<sup>160</sup> Figure 2.9a therefore shows various plausible  $fO_2$  paths of MO evolution of a growing Earth and computes the change of  $D_C^{\text{alloy/silicate}}$  along those paths, following Li et al.<sup>16</sup> It must be noted that the current data sets of  $D_C^{\text{alloy/silicate}}$  do not show any effects of pressure–temperature in relatively reducing conditions (e.g.  $\log fO_2 < IW - 1.5$ ). In such reducing conditions, the controlling variables appear to be  $fO_2$ , the Si content of the metal, and the water content of the silicate melt. At  $\sim IW - 2 < \log fO_2 < IW$ , however, the key variables controlling  $D_C^{\text{alloy/silicate}}$  are pressure, temperature,  $fO_2$ , and silicate melt composition. Figure 2.9b, however, shows that irrespective of MO condition,  $D_C^{\text{alloy/silicate}}$  remains  $\gg 1$ , and in fact deeper MO, toward the later stage of accretion, leads to even higher  $D_C^{\text{alloy/silicate}}$  predictions than those experimentally measured at shallow MO conditions. Therefore, the multistage core formation model also leads to C being stripped off highly efficiently from the silicate MO, leaving behind the BSE that is  $< 1$ –10 ppm for a bulk Earth with 1000 ppm C (Figure 2.9c).

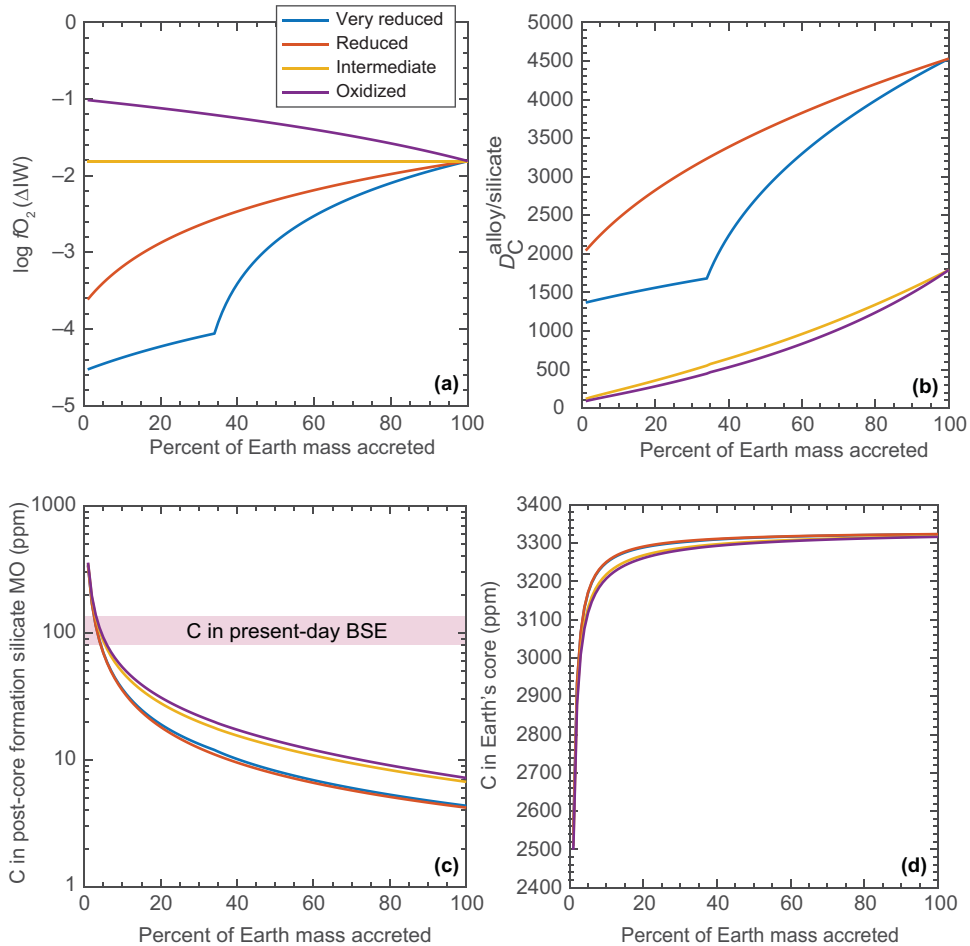


Figure 2.9 The effects of different accretion scenarios on the core–mantle partitioning behavior of carbon. (a) Four possible evolution paths for the FeO content of the mantle with its growth. The “very reduced” and “reduced” paths simulate the accretion of progressively oxidized material with time, and the “oxidized” path simulates accretion of progressively reduced material with time. All of the models converge at  $\log fO_2$  of IW – 1.8, or present-day FeO content (8 wt.%) of the primitive upper mantle. (b)  $D_C^{\text{alloy/silicate}}$  at each step of accretion (i.e. accretion of 1%  $M_E$ ), calculated using parametrized relationships from Li et al.<sup>16</sup> For the “very reduced” and “reduced” paths, where methyl (or alkyl) groups would be the predominant dissolved carbon species in the silicate melt, eq. (4) is chosen from Li et al.,<sup>16</sup> whereas for the “intermediate” and “oxidized” paths, where carbonate groups would be the predominant dissolved carbon species in the silicate melt, eq. (3) is chosen from Li et al.<sup>16</sup> (c) Post-core formation MO resulting from a bulk system with 1000 ppm C and assuming 100% alloy–silicate equilibration at each accretional step. All of the models lead to MO with distinctly less C than those estimated for the BSE. (d) Carbon content in Earth’s core converges at ~3300 ppm at the end of all accretional models.

### 2.5.3 Comparison of $D_C^{\text{alloy/silicate}}$ with Alloy–Silicate Melt Partitioning of Other LEVEs

The preceding section argues that equilibrium core formation either via homogeneous or heterogeneous accretion results in a nonmetallic Earth that is too depleted in C compared to the present-day BSE. Explaining the origin of LEVEs in the BSE through equilibrium core formation is exacerbated when  $D_C^{\text{alloy/silicate}}$  is compared with the alloy–silicate partition coefficients of other LEVEs such as S, N, and H.

The partition coefficient of sulfur between alloy and silicate melts,  $D_S^{\text{alloy/silicate}}$ , has been experimentally constrained in a number of studies,<sup>106,140,142</sup> but only a few recent studies measured  $D_S^{\text{alloy/silicate}}$  and  $D_C^{\text{alloy/silicate}}$  simultaneously.<sup>16–18</sup> These studies show that over the entire range of shallow MO conditions explored experimentally thus far,  $D_C^{\text{alloy/silicate}} \gg D_S^{\text{alloy/silicate}}$ , with  $D_C^{\text{alloy/silicate}}/D_S^{\text{alloy/silicate}}$  varying between ~1000 and 20 as  $\log fO_2$  varies from IW – 4.5 to IW – 0.5. Therefore, under any conditions of alloy–silicate equilibration, C is more siderophilic than S and equilibrium core formation leaves a subchondritic C/S ratio for the silicate MO.

Experiments also exist that constrained  $D_N^{\text{alloy/silicate}}$ .<sup>18,109,127</sup> Among these, the recent studies that constrain both  $D_C^{\text{alloy/silicate}}$  and  $D_N^{\text{alloy/silicate}}$  from the same experiments<sup>18,85</sup> show that nitrogen is only mildly siderophile in relatively oxidizing conditions and possibly even lithophile in relatively reducing conditions (e.g.  $\log fO_2 < \text{IW} - 3$ ). Therefore,  $D_C^{\text{alloy/silicate}}/D_N^{\text{alloy/silicate}}$  is ~6–120 at 1–7 GPa, 1400–1800°C, and  $fO_2$  of IW – 3.5 to IW – 0.5, and hence any models of equilibrium core formation would also produce a subchondritic C/N ratio for the post-core formation BSE.

Alloy–silicate partitioning studies for H are limited, and two available studies<sup>107,161</sup> provide contrasting data. Okuchi<sup>161</sup> estimates the  $D_H^{\text{alloy/silicate}}$  value at a fixed pressure of 7.5 GPa and as a function of temperature, but does not provide any pressure effect. Based on the experiments of Okuchi,<sup>161</sup> H is mildly siderophile. On the other hand, Clesi et al.<sup>107</sup> conducted experiments at 5, 10, and 20 GPa with C-rich alloy melts and measured  $D_H^{\text{alloy/silicate}}$  of 0.04–0.77. Therefore, it remains unclear whether H is retained mostly in the core of differentiated planets or in the silicate fraction. Despite the discrepancy in the available experimental data on  $D_H^{\text{alloy/silicate}}$ , the BSE could attain a subchondritic C/H ratio via an equilibrium core formation process where much more C would be sequestered to the metallic core than H (Figure 2.4). However, if the  $D_H^{\text{alloy/silicate}}$  data of Clesi et al.<sup>107</sup> are appropriate, then equilibrium core formation would lead to a BSE C/H ratio that is much lower than what is estimated for the present-day BSE.

## 2.6 C and Other LEVE Budgets of the BSE: A Memory of Multistage Accretion and Core Formation Process with Partial Equilibrium?

The discussion presented thus far suggests that no single process of volatile delivery such as via late accretion of any known class of meteorites or comets, through loss of an atmosphere overlying a MO,<sup>23</sup> being subjected to equilibrium core formation processes,



or sulfide segregation to the core<sup>112,162</sup> can simultaneously explain carbon's absolute as well as relative abundance compared to other LEVEs. This does not mean that these processes did not impact the volatile inventory of the BSE, and it is plausible that all of these processes acted in tandem. However, the nature of the fractionation of C with respect to H, N, and S for each of these processes is such that even if they acted together, not all of the attributes of the BSE volatile budget can be satisfied. This brings us to consider other styles of terrestrial accretion that may have been essential in establishing the LEVE budget of modern Earth.

### 2.6.1 Disequilibrium Core Formation

Models of protoplanetary disk dynamics, dust and planetesimal accretion, and planetary migration show that although the first 50% of proto-Earth mass growth was continuous, rapid, and completed within the first few million years of Solar System formation, the protracted growth of Earth spanning ~100 Myr<sup>163</sup> involved few abrupt increases in the accreted mass via several giant impacts of Mars-sized or perhaps even larger bodies.<sup>164</sup> The final such impact is thought to be the Moon-forming giant impact.<sup>165,166</sup> A key aspect of accretion via these impacts is that proto-Earth collided with differentiated planetary embryos. Merger of proto-Earth with large differentiated bodies is thought to have taken place via near-disequilibrium merger of the core of the impactor with proto-Earth's core owing to limited emulsification of the impactor's core and the lack of complete mixing of the core with the entrained silicate melt.<sup>167,168</sup> Therefore, core formation involving giant impacts may leave a silicate fraction with a very different LEVE budget than that predicted by equilibrium core formation models. One critical question is whether any differentiated, large impactor could bring LEVE attributes that would help proto-Earth to evolve to the present-day BSE. A full-parameter space involving not only the LEVEs but also other nonvolatile, highly siderophile, and moderately siderophile elements, major elements, and stable isotope anomalies, as well as various accretion and core formation model assumptions, is not yet explored. However, recent studies<sup>16–18</sup> showed how having an S-rich or Si-rich Fe-alloy in the cores of planetary embryos allow attaining high C/N and C/S ratios in the mantles of such embryos. This would occur as the cores of these embryos reach the C solubility limit and expel graphite or diamond to the overlying silicate fraction (Figure 2.10).<sup>16–18</sup> Therefore, a merger of the silicate reservoirs of such embryos with the proto-silicate Earth reservoir could give rise to the BSE LEVE inventory. Using inverse Monte Carlo simulations, Grewal et al.<sup>18</sup> showed that if the merger of the impactor is in perfect disequilibrium, depending on the core size of the impactor and bulk S content, the impactor could be similar in size as Mars (~0.1 M<sub>E</sub>; Figure 2.10). It is also showed that the bulk C content of such an impactor would not need to be enriched in carbon and could have a bulk C concentration (~1000–5000 ppm C)<sup>17,18</sup> similar to those of E-chondrites. These model results are intriguing because these potentially circumvent the long-standing challenge of reconciling the volatile element isotope constraints<sup>51,59</sup> and constraints from the isotopic anomalies of lithophile and siderophile elements<sup>31,32</sup> in the major building blocks

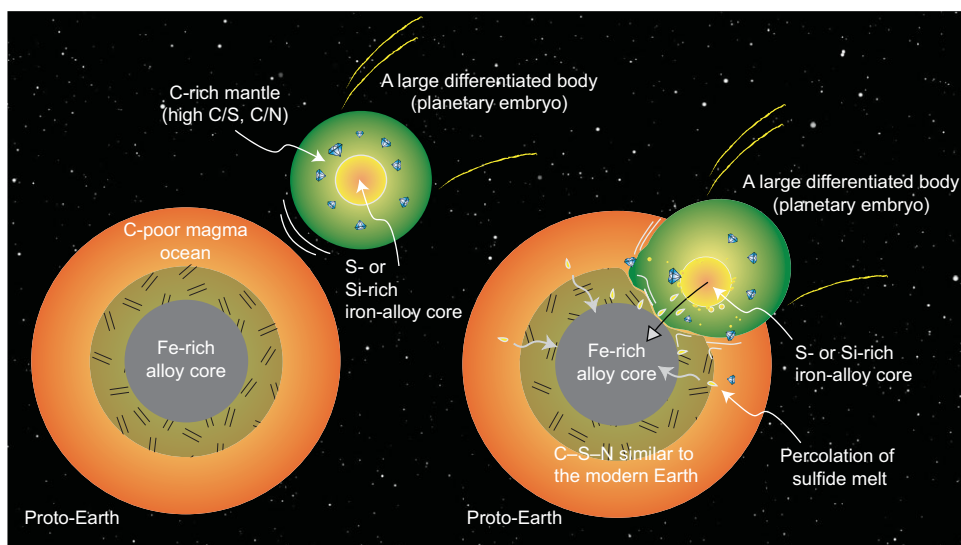


Figure 2.10 A schematic depiction of the late-stage accretion for a large rocky planet such as Earth where a large fraction of mass increase takes place via giant impacts of small planets and planetary embryos ( $0.1\text{--}0.2\text{ M}_{\text{E}}$ ).<sup>16–18</sup> This mode of accretion creates a unique possibility of establishing the LEVE inventory in the degassable portion of the rocky planets.

of Earth. Some of these latest studies on the origins of terrestrial volatiles through late-stage accretion of a differentiated planetary embryo are also conceptually similar to models that call for the addition of a highly reduced rocky body to the growing Earth to potentially explain the superchondritic Sm/Nd and  $^{142}\text{Nd}/^{144}\text{Nd}$  anomalies observed in Earth's present mantle.<sup>169,170</sup> The concept of bringing carbon and other LEVEs via accretion of the mantle of a differentiated embryo with little post-impact equilibration is also similar to the suggestion that Earth's Nb/Ta may be explained by accretion of a differentiated asteroid with a reduced S-rich core that efficiently sequestered Nb.<sup>171</sup> Grewal et al.<sup>18</sup> also posited that Earth's volatile-delivering impactor may have been the Moon-forming giant impactor, given the geochemical similarity, including volatiles, between the BSE and the Moon. This is again broadly consistent with Wade and Wood,<sup>172</sup> who demonstrated that near-disequilibrium accretion of a reduced planetary embryo of  $0.1\text{--}0.2\text{ M}_{\text{E}}$  could explain the isotopic constraints, FeO contents, and Nb/Ta and Hf/W ratios of the silicate Earth and Moon.

## 2.7 Carbon as a Light Element in the Core

One by-product of our discussion thus far is constraint on the concentration of C in the core. One of the main uncertainties in constraining the C budget of Earth's core is the bulk C content in the growing Earth through time in the first  $\sim 100\text{--}120\text{ Myr}$  of the Solar System.

It is not realistic to conceive that Earth's building blocks and therefore the bulk C content did not change through the accretion history, but for simplicity here we assume a fixed C budget for the entire history of core formation or MO equilibration. If core formation was achieved by a single-stage equilibrium event at a deep MO, although not a physically realistic process, C content in the core as shown by Dasgupta<sup>8</sup> would be ~0.2 wt.% for a bulk Earth C content of ~730–1000 ppm. For a multistage core formation, with evolving depth–temperature– $f\text{O}_2$  conditions of alloy–silicate equilibration, the core would finally contain ~0.34 wt.% C (Figure 2.9d). Finally, in the model where the C–N–S budget of the BSE is attained via late-stage merger of a large differentiated planetary embryo, the impactor's S-rich core contributes ~100–700 ppm C to Earth's core.<sup>17,18</sup> Therefore, depending on the volatile budget of the growing Earth leading to the giant impact, from a completely C-free proto-Earth to a proto-Earth with 1000 ppm bulk C, the final core C content would be between 700 ppm and 0.4 wt.%. The upper bound derived here is similar to the previous constraint<sup>14</sup> placed using the mantle C abundance. Wood et al.<sup>60</sup> also attempted to place constraint on the C content of Earth's core based on the combined effects of C and S in the alloy on alloy–silicate partitioning of W and Mo, with the chief effect being W and Mo becoming more siderophile with increasing C in the alloy melt. By coupling S and C delivery in the final 13% of accretion, Wood et al.<sup>60</sup> showed that in order to obtain the known Mo and W abundances of the mantle, the bulk C content of the core needs to be <1 wt.%. Badro et al.<sup>160</sup> also reached a similar conclusion that, in order to simultaneously satisfy the geochemical and geophysical constraints, Earth's core composition cannot contain C as one of the major light elements. Therefore, all of the constraints thus far point to Earth's core being the largest C reservoir, yet C being a minor light element in the core.

## 2.8 Conclusion

The origins of Earth's LEVEs, including C, remain debated. Such debate stems in part from the uncertainty regarding the whole-Earth budget of C and other volatile elements and in part from the fate of these elements in putative planetary building blocks throughout their journey in the protoplanetary disk and planet formation process. While the abundance of each LEVE in the BSE is poorly constrained, the ratios of various LEVEs (along with their isotopic compositions) are more reliable geochemical indices to isolate key processes. Some of the key processes to consider are the accretion of undifferentiated chondritic meteorites, compound-specific condensation of the LEVEs, fractionation of the LEVEs during alloy–silicate differentiation, and MO–proto-atmosphere partitioning aided by redox-controlled solubility. Probing each of these processes in the light of the evolution of the LEVE ratios suggests that no single process or combination of processes can result in the currently estimated abundance of LEVEs in the BSE. However, a new paradigm is emerging where the late-stage growth of Earth via the impact and accretion of differentiated planetary embryos (0.1–0.2  $M_E$ ) may not only explain the abundances of C–N–S, but also satisfy

the broad geochemical similarity of Earth and the Moon. Despite the similarity in the arguments put forward by many recent studies that call for the accretion of one or more large planetary embryos with little post-impact equilibration of the impactor's core with the terrestrial mantle/MO, differences remain in their details. For example, Grewal et al.<sup>18</sup> proposed accretion of a relatively oxidized planet with an S-rich core, whereas Wade and Wood<sup>172</sup> called for accretion of a reduced planet with S-rich core. Future studies, therefore, will have to investigate how to reconcile these differences while fulfilling all of the geochemical constraints, both for non-volatile lithophile and siderophile elements and LEVEs. Nonetheless, it appears inevitable that a large planet like Earth's LEVE budgets were shaped by its protracted growth history with episodes of planetesimals, planetary embryos, and planet accretion, whereas other smaller planets that grew quickly lacked some of these possible supply and modification mechanisms of key ingredients. Whatever the accretion mechanism may be, as long as mostly volatile-depleted materials accreted on Earth throughout its core formation history, C as well as N and H are going to be minor elements in the bulk core. As the search continues to find other rocky, habitable worlds beyond our Solar System, the origins of C–H–N–S on Earth provide a guiding framework.

## 2.9 Limits of Knowledge and Unknowns

The limits of knowledge on the origin of Earth's C and other LEVEs derive from current unknowns about many fundamental questions regarding the formation and evolution of Earth and other rocky planets in the Solar System, as well as about the compositions and processes in Earth's deep interior. The condensation temperature of C that dictates the formation of solid C-bearing compounds from gases is thought to be extremely low,<sup>173</sup> leading to the idea that most C brought to the inner Solar System at the early stage of planet formation is largely lost from the building blocks. However, it remains unknown whether some of the refractory C-bearing phases such as graphite and carbide could have contributed to the C budget of Earth during its early growth stage.

Experimental data on alloy–silicate elemental partitioning for mixed-volatile systems, especially in conditions approaching the deep MO of Earth, are still lacking and are needed in order to refine some of the current ideas based on extrapolated values from relatively low pressure–temperature experiments. Similar experimental data are needed for volatile isotopic systems as well, which are even more restricted,<sup>174,175</sup> and for many systems, such as C,<sup>64</sup> H, and S,<sup>175</sup> they are either nonexistent or do not extend to the pressure–temperature and compositional space directly relevant for MOs.

## Acknowledgments

The authors thank many former and current members of Rice University's experimental petrology team, including Han Chi, Yuan Li, Megan Duncan, Alexandra Holmes, Kyusei Tsuno, and James Eguchi, whose research results influenced the views expressed in this

chapter. The authors thank Jonathan Tucker and coeditor Isabelle Daniel for useful reviews. This work was made possible by funding from NASA grants 80NSSC18K0828 and 80NSSC18K1314, the Deep Carbon Observatory, and a Packard Fellowship for Science and Engineering to RD.

### Questions for the Classroom

- 1 How well do the chondritic meteorites (undifferentiated materials; i.e. mixtures or metals, sulfides, and silicates), derived from the main asteroid belt, represent the building blocks of Earth and other rocky planets and planetary embryos in the inner Solar System? In other words, should the plausible compositions of building blocks including their LEVE budgets remain restricted to the known classes of meteorites?
- 2 How could we improve our knowledge on the concentration of C, N, S, and H in the BSE? What other approaches can be used to determine the mantle inventory of LEVEs?
- 3 How can we improve our understanding of the relative contributions of giant impacts versus impacts of planetesimals on the acquisition of LEVEs for large, rocky planets?
- 4 What information from our knowledge on the origins of LEVEs on Earth can be applied to build a framework for exoplanetary chemical habitability?

### References

1. Birch, F., Elasticity and constitution of the Earth's interior. *J. Geophys. Res.* **57**, 227–286 (1952).
2. Birch, F., Density and composition of mantle and core. *J. Geophys. Res.* **69**, 4377–4388 (1964).
3. Poirier, J.-P., Light elements in the Earth's outer core: a critical review. *Phys. Earth Planet. Int.* **85**, 319–337 (1994).
4. Javoy, M., Pineau, F., & Allègre, C.J., Carbon geodynamic cycle. *Nature* **300**, 171–173 (1982).
5. Sleep, N.H. & Zahnle, K., Carbon dioxide cycling and implications for climate on ancient earth. *J. Geophys. Res.* **106**, 1373–1399 (2001).
6. Hayes, J.F. & Waldbauer, J.R., The carbon cycle and associated redox processes through time. *Phil. Trans. Royal Soc. London* **B361**, 931–950 (2006).
7. Hirschmann, M.M. & Dasgupta, R., The H/C ratios of Earth's near-surface and deep reservoirs, and consequences for deep Earth volatile cycles. *Chem. Geol.* **262**, 4–16 (2009).
8. Dasgupta, R., Ingassing, storage, and outgassing of terrestrial carbon through geologic time. *Rev. Min. Geochem.* **75**, 183–229 (2013).
9. Dasgupta, R. & Hirschmann, M.M., The deep carbon cycle and melting in Earth's interior. *Earth Planet. Sci. Lett.* **298**, 1–13 (2010).
10. Bergin, E.A., Blake, G.A., Ciesla, F., Hirschmann, M.M., & Li, J., Tracing the ingredients for a habitable earth from interstellar space through planet formation. *Proc. Natl Acad. Sci.* **112**, 8965–8970 (2015).
11. Hirschmann, M.M., Constraints on the early delivery and fractionation of Earth's major volatiles from C/H, C/N, and C/S ratios. *Am. Mineral.* **101**, 540–553 (2016).

12. Halliday, A.N., The origins of volatiles in the terrestrial planets. *Geochim. Cosmochim. Acta* **105**, 146–171 (2013).
13. Marty, B., The origins and concentrations of water, carbon, nitrogen and noble gases on Earth. *Earth Planet. Sci. Lett.* **313–314**, 56–66 (2012).
14. Dasgupta, R. & Walker, D., Carbon solubility in core melts in a shallow magma ocean environment and distribution of carbon between the Earth's core and the mantle. *Geochim. Cosmochim. Acta* **72**, 4627–4641 (2008).
15. Kuramoto, K. & Matsui, T., Partitioning of H and C between the mantle and core during the core formation in the Earth: its implications for the atmospheric evolution and redox state of early mantle. *J. Geophys. Res.* **101**, 14909–14932 (1996).
16. Li, Y., Dasgupta, R., Tsuno, K., Monteleone, B., & Shimizu, N., Carbon and sulfur budget of the silicate Earth explained by accretion of differentiated planetary embryos. *Nat. Geosci.* **9**, 781–785 (2016).
17. Tsuno, K., Grewal, D.S., & Dasgupta, R., Core–mantle fractionation of carbon in Earth and Mars: the effects of sulfur. *Geochim. Cosmochim. Acta* **238**, 477–495 (2018).
18. Grewal, D.S., Dasgupta, R., Sun, C., Tsuno, K., & Costin, G., Delivery of carbon, nitrogen and sulfur to the silicate Earth by a giant impact. *Science Adv.* **5**, eaau3669 (2019).
19. Morbidelli, A., Lunine, J.I., O'Brien, D.P., Raymond, S.N., & Walsh, K.J., Building terrestrial planets. *Ann. Rev. Earth Planet. Sci.* **40**, 251–275 (2012).
20. O'Brien, D.P., Walsh, K.J., Morbidelli, A., Raymond, S.N., & Mandell, A.M., Water delivery and giant impacts in the “Grand Tack” scenario. *Icarus* **239**, 74–84 (2014).
21. Marchi, S., Canup, R.M., & Walker, R.J., Heterogeneous delivery of silicate and metal to the Earth by large planetesimals. *Nat. Geosci.* **11**, 77–81 (2018).
22. Schlichting, H.E. & Mukhopadhyay, S., Atmosphere impact losses. *Space Sci. Rev.* **214**, 34 (2018).
23. Schlichting, H.E., Sari, R.E., & Yalinewich, A., Atmospheric mass loss during planet formation: the importance of planetesimal impacts. *Icarus* **247**, 81–94 (2015).
24. Ahrens, T.J., Impact erosion of terrestrial planetary atmospheres. *Ann. Rev. Earth Planet. Sci.* **21**, 525–555 (1993).
25. Ringwood, A.E., Chemical evolution of the terrestrial planets. *Geochim. Cosmochim. Acta* **30**, 41–104 (1966).
26. Anders, E. & Ebihara, M., Solar-system abundances of the elements. *Geochim. Cosmochim. Acta* **46**, 2363–2380 (1982).
27. Allègre, C., Manhès, G., & Lewin, É., Chemical composition of the Earth and the volatility control on planetary genetics. *Earth Planet. Sci. Lett.* **185**, 49–69 (2001).
28. Clayton, R.N., Onuma, N., & Mayeda, T.K., A classification of meteorites based on oxygen isotopes. *Earth Planet. Sci. Lett.* **30**, 10–18 (1976).
29. Clayton, R.N., Oxygen isotopes in meteorites. *Ann. Rev. Earth Planet. Sci.* **21**, 115–149 (1993).
30. Young, E.D. et al., Oxygen isotopic evidence for vigorous mixing during the Moon-forming giant impact. *Science* **351**, 493–496 (2016).
31. Dauphas, N. et al., Calcium-48 isotopic anomalies in bulk chondrites and achondrites: evidence for a uniform isotopic reservoir in the inner protoplanetary disk. *Earth Planet. Sci. Lett.* **407**, 96–108 (2014).
32. Dauphas, N., The isotopic nature of the Earth's accreting material through time. *Nature* **541**, 521 (2017).
33. Fischer-Gödde, M. & Kleine, T., Ruthenium isotopic evidence for an inner Solar System origin of the late veneer. *Nature* **541**, 525 (2017).



34. Javoy, M. et al., The chemical composition of the Earth: enstatite chondrite models. *Earth Planet. Sci. Lett.* **293**, 259–268 (2010).
35. Javoy, M., The integral enstatite chondrite model of the Earth. *Geophys. Res. Lett.* **22**, 2219–2222 (1995).
36. McDonough, W.F. & Sun, S.-S., The composition of the Earth. *Chem. Geol.* **120**, 223–253 (1995).
37. Wasson, J.T. & Kallemeyn, G.W., Compositions of chondrites. *Phil. Trans. Royal Soc. A.* **325**, 535–544 (1988).
38. Fitoussi, C., Bourdon, B., & Wang, X., The building blocks of Earth and Mars: a close genetic link. *Earth Planet. Sci. Lett.* **434**, 151–160 (2016).
39. Palme, H. & O'Neill, H.S.C., Cosmochemical estimates of mantle composition, in *The Mantle and Core*, Vol. 2, ed. R.W. Carlson (Oxford: Pergamon Press, 2007), pp. 1–38.
40. Murakami, M., Ohishi, Y., Hirao, N., & Hirose, K., A perovskitic lower mantle inferred from high-pressure, high-temperature sound velocity data. *Nature* **485**, 90 (2012).
41. Fitoussi, C. & Bourdon, B., Silicon isotope evidence against an enstatite chondrite Earth. *Science* **335**, 1477–1480 (2012).
42. Shahar, A. et al., Experimentally determined Si isotope fractionation between silicate and Fe metal and implications for Earth's core formation. *Earth Planet. Sci. Lett.* **288**, 228–234 (2009).
43. Shahar, A. et al., High-temperature Si isotope fractionation between iron metal and silicate. *Geochim. Cosmochim. Acta* **75**, 7688–7697 (2011).
44. Ballmer, M.D., Houser, C., Hernlund, J.W., Wentzcovitch, R.M., & Hirose, K., Persistence of strong silica-enriched domains in the Earth's lower mantle. *Nat. Geosci.* **10**, 236 (2017).
45. Dauphas, N., Poitrasson, F., Burkhardt, C., Kobayashi, H., & Kurosawa, K., Planetary and meteoritic Mg/Si and  $\delta^{30}\text{Si}$  variations inherited from solar nebula chemistry. *Earth Planet. Sci. Lett.* **427**, 236–248 (2015).
46. McNaughton, N.J., Borthwick, J., Fallick, A.E., & Pillinger, C.T., Deuterium/hydrogen ratios in unequilibrated ordinary chondrites. *Nature* **294**, 639 (1981).
47. Robert, F., Merlivat, L., & Javoy, M., Deuterium concentration in the early Solar System: hydrogen and oxygen isotope study. *Nature* **282**, 785 (1979).
48. Alexander, C.M.O.D. et al., The provenances of asteroids, and their contributions to the volatile inventories of the terrestrial planets. *Science* **337**, 721–723 (2012).
49. Pearson, V.K., Sephton, M.A., Franchi, I.A., Gibson, J.M., & Gilmour, I., Carbon and nitrogen in carbonaceous chondrites: elemental abundances and stable isotopic compositions. *Meteor. Planet. Sci.* **41**, 1899–1918 (2006).
50. Marty, B., Alexander, C.M.O.D., & Raymond, S., Primordial origins of Earth's carbon. *Rev. Mineral. Geochem.* **75**, 149–181 (2013).
51. Sarafian, A.R., Nielsen, S.G., Marschall, H.R., McCubbin, F.M., & Monteleone, B.D., Early accretion of water in the inner solar system from a carbonaceous chondrite-like source. *Science* **346**, 623–626 (2014).
52. Grady, M.M., Wright, I.P., Carr, L.P., & Pillinger, C.T., Compositional differences in enstatite chondrites based on carbon and nitrogen stable isotope measurements. *Geochim. Cosmochim. Acta* **50**, 2799–2813 (1986).
53. Alexander, C.M.O.D., Swan, P., & Prombo, C.A., Occurrence and implications of silicon nitride in enstatite chondrites. *Meteor. Planet. Sci.* **29**, 79–85 (1994).



54. Alexander, C.M.O.D., McKeegan, K.D., & Altwegg, K., Water reservoirs in small planetary bodies: meteorites, asteroids, and comets. *Space Sci. Rev.* **214**, 36 (2018).
55. Sarafian, A.R. et al., Early accretion of water and volatile elements to the inner Solar System: evidence from angrites. *Phil. Trans. Royal Soc. A.* **375**, 20160209 (2017).
56. Geiss, J. & Gloeckler, G., Isotopic composition of H, HE and NE in the protosolar cloud. *Space Sci. Rev.* **106**, 3–18 (2003).
57. Ko, H., Marc, C., Bernard, M., & Kentaro, T., Protosolar carbon isotopic composition: implications for the origin of meteoritic organics. *Astrophys. J.* **600**, 480 (2004).
58. Marty, B., Chaussidon, M., Wiens, R.C., Jurewicz, A.J.G., & Burnett, D.S., A  $^{15}\text{N}$ -poor isotopic composition for the Solar System as shown by genesis solar wind samples. *Science* **332**, 1533–1536 (2011).
59. Marty, B. & Yokochi, R., Water in the early Earth. *Rev. Mineral. Geochem.* **62**, 421–450 (2006).
60. Wood, B.J., Li, J., & Shahar, A., Carbon in the core: its influence on the properties of core and mantle. *Rev. Mineral. Geochem.* **75**, 231–250 (2013).
61. Kerridge, J.F., Carbon, hydrogen and nitrogen in carbonaceous chondrites: abundances and isotopic compositions in bulk samples. *Geochim. Cosmochim. Acta* **49**, 1707–1714 (1985).
62. Deines, P., The carbon isotope geochemistry of mantle xenoliths. *Earth Sci. Rev.* **58**, 247–278 (2002).
63. Labidi, J., Cartigny, P., & Moreira, M., Non-chondritic sulphur isotope composition of the terrestrial mantle. *Nature* **501**, 208 (2013).
64. Satish-Kumar, M., So, H., Yoshino, T., Kato, M., & Hiroi, Y., Experimental determination of carbon isotope fractionation between iron carbide melt and carbon:  $^{12}\text{C}$ -enriched carbon in the Earth's core? *Earth Planet. Sci. Lett.* **310**, 340–348 (2011).
65. Walsh, K.J., Morbidelli, A., Raymond, S.N., O'Brien, D.P., & Mandell, A.M., A low mass for Mars from Jupiter's early gas-driven migration. *Nature* **475**, 206–209 (2011).
66. Raymond, S.N., O'Brien, D.P., Morbidelli, A., & Kaib, N.A., Building the terrestrial planets: constrained accretion in the inner Solar System. *Icarus* **203**, 644–662 (2009).
67. Dauphas, N. & Pourmand, A., Hf–W–Th evidence for rapid growth of Mars and its status as a planetary embryo. *Nature* **473**, 489–492 (2011).
68. Lambrechts, M. & Johansen, A., Rapid growth of gas-giant cores by pebble accretion. *Astronom. Astrophys.* **544**, A32 (2012).
69. Johansen, A., Low, M.-M.M., Lacerda, P., & Bizzarro, M., Growth of asteroids, planetary embryos, and Kuiper belt objects by chondrule accretion. *Sci. Adv.* **1**, e1500109 (2015).
70. Wetzel, D.T., Hauri, E.H., Saal, A.E., & Rutherford, M.J., Carbon content and degassing history of the lunar volcanic glasses. *Nat. Geosci.* **8**, 755–758 (2015).
71. Chi, H., Dasgupta, R., Duncan, M., & Shimizu, N., Partitioning of carbon between Fe-rich alloy melt and silicate melt in a magma ocean – implications for the abundance and origin of volatiles in Earth, Mars, and the Moon. *Geochim. Cosmochim. Acta* **139**, 447–471 (2014).
72. Saal, A.E. et al., Volatile content of lunar volcanic glasses and the presence of water in the Moon's interior. *Nature* **454**, 192–195 (2008).
73. Hauri, E.H., Weinreich, T., Saal, A.E., Rutherford, M.C., & Van Orman, J.A., High pre-eruptive water contents preserved in lunar melt inclusions. *Science* **333**, 213–215 (2011).

74. Saal, A.E., Hauri, E.H., Van Orman, J.A., & Rutherford, M.J., Hydrogen isotopes in lunar volcanic glasses and melt inclusions reveal a carbonaceous chondrite heritage. *Science* **340**, 1317–1320 (2013).
75. Greenwood, R.C. et al., Oxygen isotopic evidence for accretion of Earth's water before a high-energy Moon-forming giant impact. *Sci. Adv.* **4**, eaao5928 (2018).
76. Palme, H., Lodders, K., & Jones, A., Solar system abundances of the elements, in *Treatise on Geochemistry (2nd edn.)*, eds. H.D. Holland & K.K. Turekian (Oxford: Elsevier, 2014), pp. 15–36.
77. Anders, E. & Grevesse, N., Abundances of the elements: meteoritic and solar. *Geochim. Cosmochim. Acta* **53**, 197–214 (1989).
78. Lodders, K., Solar system abundances of the elements, in *Principles and Perspectives in Cosmochemistry: Lecture Notes of the Kodai School on "Synthesis of Elements in Stars"*, eds. A. Goswami & B. Eswar Reddy (Berlin: Springer-Verlag, 2010), pp. 379–417.
79. Palme, H. & Jones, A., Solar system abundances of the elements, in *Meteorites, Comets, and Planets*, ed. A.M. Davis (Amsterdam: Elsevier Ltd., 2003), pp. 41–61.
80. Grady, M.M. & Wright, I.P., Elemental and isotopic abundances of carbon and nitrogen in meteorites. *Space Sci. Rev.* **106**, 231–248 (2003).
81. Hutson, M. & Ruzicka, A., A multi-step model for the origin of E3 (enstatite) chondrites. *Meteor. Planet. Sci.* **35**, 601–608 (2000).
82. Hirschmann, M.M., Water, melting, and the deep Earth H<sub>2</sub>O cycle. *Ann. Rev. Earth Planet. Sci.* **34**, 629–653 (2006).
83. McDonough, W.F., Compositional model for the Earth's core, in *The Mantle and Core, Vol. 2*, ed. R.W. Carlson (Oxford: Elsevier-Pergamon, 2003), pp. 547–568.
84. Rosenthal, A., Hauri, E.H., & Hirschmann, M.M., Experimental determination of C, F, and H partitioning between mantle minerals and carbonated basalt, CO<sub>2</sub>/Ba and CO<sub>2</sub>/Nb systematics of partial melting, and the CO<sub>2</sub> contents of basaltic source regions. *Earth Planet. Sci. Lett.* **412**, 77–87 (2015).
85. Dalou, C., Hirschmann, M.M., von der Handt, A., Mosenfelder, J., & Armstrong, L.S., Nitrogen and carbon fractionation during core–mantle differentiation at shallow depth. *Earth Planet. Sci. Lett.* **458**, 141–151 (2017).
86. Nabiei, F. et al., A large planetary body inferred from diamond inclusions in a ureilite meteorite. *Nat. Commun.* **9**, 1327 (2018).
87. Kana, N., Masayuki, N., & Jun-ichi, M., Raman spectroscopic study of diamond and graphite in ureilites and the origin of diamonds. *Meteor. Planet. Sci.* **47**, 1728–1737 (2012).
88. Barrat, J.-A., Sansjofre, P., Yamaguchi, A., Greenwood, R.C., & Gillet, P., Carbon isotopic variation in ureilites: evidence for an early, volatile-rich inner Solar System. *Earth Planet. Sci. Lett.* **478**, 143–149 (2017).
89. Schiller, M., Bizzarro, M., & Fernandes, V.A., Isotopic evolution of the protoplanetary disk and the building blocks of Earth and the Moon. *Nature* **555**, 507 (2018).
90. Ding, S. & Dasgupta, R., The fate of sulfide during decompression melting of peridotite – implications for sulfur inventory of the MORB-source depleted upper mantle. *Earth Planet. Sci. Lett.* **459**, 183–195 (2017).
91. Saal, A.E., Hauri, E., Langmuir, C.H., & Perfit, M.R., Vapour undersaturation in primitive mid-ocean-ridge basalt and the volatile content of Earth's upper mantle. *Nature* **419**, 451–455 (2002).
92. Rehkämper, M. et al., Ir, Ru, Pt, and Pd in basalts and komatiites: new constraints for the geochemical behavior of the platinum-group elements in the mantle. *Geochim. Cosmochim. Acta* **63**, 3915–3934 (1999).

93. Walker, R.J., Highly siderophile elements in the Earth, Moon and Mars: update and implications for planetary accretion and differentiation. *Geochemistry* **69**, 101–125 (2009).
94. Mann, U., Frost, D.J., Rubie, D.C., Becker, H., & Audétat, A., Partitioning of Ru, Rh, Pd, Re, Ir and Pt between liquid metal and silicate at high pressures and high temperatures – implications for the origin of highly siderophile element concentrations in the Earth’s mantle. *Geochim. Cosmochim. Acta* **84**, 593–613 (2012).
95. Morgan, J.W., Walker, R.J., Brandon, A.D., & Horan, M.F., Siderophile elements in Earth’s upper mantle and lunar breccias: data synthesis suggests manifestations of the same late influx. *Meteor. Planet. Sci.* **36**, 1257–1275 (2001).
96. Willbold, M., Elliott, T., & Moorbath, S., The tungsten isotopic composition of the Earth’s mantle before the terminal bombardment. *Nature* **477**, 195 (2011).
97. Albarede, F., Volatile accretion history of the terrestrial planets and dynamic implications. *Nature* **461**, 1227–1233 (2009).
98. Albarede, F. et al., Asteroidal impacts and the origin of terrestrial and lunar volatiles. *Icarus* **222**, 44–52 (2013).
99. Dasgupta, R., Chi, H., Shimizu, N., Buono, A., & Walker, D., Carbon solution and partitioning between metallic and silicate melts in a shallow magma ocean: implications for the origin and distribution of terrestrial carbon. *Geochim. Cosmochim. Acta* **102**, 191–212 (2013).
100. Alexander, C.M.O.D., Fogel, M., Yabuta, H., & Cody, G.D., The origin and evolution of chondrites recorded in the elemental and isotopic compositions of their macromolecular organic matter. *Geochim. Cosmochim. Acta* **71**, 4380–4403 (2007).
101. Vdovykin, G.P., Ureilites. *Space Sci. Rev.* **10**, 483–510 (1970).
102. Grady, M.M., Wright, I.P., Swart, P.K., & Pillinger, C.T., The carbon and nitrogen isotopic composition of ureilites: implications for their genesis. *Geochim. Cosmochim. Acta* **49**, 903–915 (1985).
103. Downes, H. et al., Isotopic composition of carbon and nitrogen in ureilitic fragments of the Almahata Sitta meteorite. *Meteor. Planet. Sci.* **50**, 255–272 (2015).
104. Siebert, J., Badro, J., Antonangeli, D., & Ryerson, F.J., Metal–silicate partitioning of Ni and Co in a deep magma ocean. *Earth Planet. Sci. Lett.* **321–322**, 189–197 (2012).
105. Grewal, D.S., Dasgupta, R., Holmes, A.K., Costin, G., & Li, Y., The fate of nitrogen during core–mantle separation on Earth. *Geochim. Cosmochim. Acta* **251**, 87–115 (2019).
106. Boujibar, A. et al., Metal–silicate partitioning of sulphur, new experimental and thermodynamic constraints on planetary accretion. *Earth Planet. Sci. Lett.* **391**, 42–54 (2014).
107. Clesi, V. et al., Low hydrogen contents in the cores of terrestrial planets. *Science Adv.* **4**, e1701876 (2018).
108. Armstrong, L.S., Hirschmann, M.M., Stanley, B.D., Falksen, E.G., & Jacobsen, S.D., Speciation and solubility of reduced C–O–H–N volatiles in mafic melt: implications for volcanism, atmospheric evolution, and deep volatile cycles in the terrestrial planets. *Geochim. Cosmochim. Acta* **171**, 283–302 (2015).
109. Roskosz, M., Bouhifd, M.A., Jephcoat, A.P., Marty, B., & Mysen, B.O., Nitrogen solubility in molten metal and silicate at high pressure and temperature. *Geochim. Cosmochim. Acta* **121**, 15–28 (2013).

110. O'Neill, H.S.C. & Mavrogenes, J.A., The sulfide capacity and the sulfur content at sulfide saturation of silicate melts at 1400°C and 1 bar. *J. Petrol.* **43**, 1049–1087 (2002).
111. Hirschmann, M.M., Withers, A.C., Ardia, P., & Foley, N.T., Solubility of molecular hydrogen in silicate melts and consequences for volatile evolution of terrestrial planets. *Earth Planet. Sci. Lett.* **345**, 38–48 (2012).
112. Rubie, D.C. et al., Highly siderophile elements were stripped from Earth's mantle by iron sulfide segregation. *Science* **353**, 1141–1144 (2016).
113. Corgne, A., Wood, B.J., & Fei, Y., C- and S-rich molten alloy immiscibility and core formation of planetesimals. *Geochim. Cosmochim. Acta* **72**, 2409–2416 (2008).
114. Dasgupta, R., Buono, A., Whelan, G., & Walker, D., High-pressure melting relations in Fe–C–S systems: implications for formation, evolution, and structure of metallic cores in planetary bodies. *Geochim. Cosmochim. Acta* **73**, 6678–6691 (2009).
115. Tsuno, K. & Dasgupta, R., Fe–Ni–Cu–C–S phase relations at high pressures and temperatures – the role of sulfur in carbon storage and diamond stability at mid- to deep-upper mantle. *Earth Planet. Sci. Lett.* **412**, 132–142 (2015).
116. Zhang, Z., Hastings, P., Von der Handt, A., & Hirschmann, M.M., Experimental determination of carbon solubility in Fe–Ni–S melts. *Geochim. Cosmochim. Acta* **225**, 66–79 (2018).
117. Li, Y., Dasgupta, R., & Tsuno, K., The effects of sulfur, silicon, water, and oxygen fugacity on carbon solubility and partitioning in Fe-rich alloy and silicate melt systems at 3 GPa and 1600°C: implications for core–mantle differentiation and degassing of magma oceans and reduced planetary mantles. *Earth Planet. Sci. Lett.* **415**, 54–66 (2015).
118. Raymond, S.N., Quinn, T., & Lunine, J.I., High-resolution simulations of the final assembly of Earth-like planets. 2. Water delivery and planetary habitability. *Astrobiology* **7**, 66–84 (2007).
119. Hallis, L.J. et al., Evidence for primordial water in Earth's deep mantle. *Science* **350**, 795–797 (2015).
120. Tucker, J.M. & Mukhopadhyay, S., Evidence for multiple magma ocean outgassing and atmospheric loss episodes from mantle noble gases. *Earth Planet. Sci. Lett.* **393**, 254–265 (2014).
121. Kress, V.C. & Carmichael, I.S.E., The compressibility of silicate liquids containing Fe<sub>2</sub>O<sub>3</sub> and the effect of composition, temperature, oxygen fugacity and pressure on their redox states. *Contrib. Mineral. Petrol.* **108**, 82–92 (1991).
122. O'Neill, H.S.C. et al., An experimental determination of the effect of pressure on the Fe<sup>3+</sup>/ΣFe ratio of an anhydrous silicate melt to 3.0 GPa. *Am. Mineral.* **91**, 404–412 (2006).
123. Zhang, H.L., Hirschmann, M.M., Cottrell, E., & Withers, A.C., Effect of pressure on Fe<sup>3+</sup>/ΣFe ratio in a mafic magma and consequences for magma ocean redox gradients. *Geochim. Cosmochim. Acta* **204**, 83–103 (2017).
124. Schaefer, L. & Elkins-Tanton, L.T., Magma oceans as a critical stage in the tectonic development of rocky planets. *Phil. Trans. Royal Soc. A* **376**, 20180109 (2018).
125. Duncan, M.S., Dasgupta, R., & Tsuno, K., Experimental determination of CO<sub>2</sub> content at graphite saturation along a natural basalt–peridotite melt join: implications for the fate of carbon in terrestrial magma oceans. *Earth Planet. Sci. Lett.* **466**, 115–128 (2017).
126. Libourel, G., Marty, B., & Humbert, F., Nitrogen solubility in basaltic melt. Part I. Effect of oxygen fugacity. *Geochim. Cosmochim. Acta* **67**, 4123–4135 (2003).

127. Kadik, A.A. et al., Influence of oxygen fugacity on the solubility of nitrogen, carbon, and hydrogen in  $\text{FeO-Na}_2\text{O-SiO}_2\text{-Al}_2\text{O}_3$  melts in equilibrium with metallic iron at 1.5 GPa and 1400°C. *Geochem. Int.* **49**, 429–438 (2011).
128. Holloway, J.R., Pan, V., & Gudmundsson, G., High-pressure fluid-absent melting experiments in the presence of graphite; oxygen fugacity, ferric/ferrous ratio and dissolved  $\text{CO}_2$ . *Eur. J. Mineral.* **4**, 105–114 (1992).
129. Li, Y., Dasgupta, R., & Tsuno, K., Carbon contents in reduced basalts at graphite saturation: implications for the degassing of Mars, Mercury, and the Moon. *J. Geophys. Res. Planets* **122**, doi:10.1002/2017JE005289 (2017).
130. Ding, S., Hough, T., & Dasgupta, R., New high pressure experiments on sulfide saturation of high-FeO\* basalts with variable  $\text{TiO}_2$  contents – implications for the sulfur inventory of the lunar interior. *Geochim. Cosmochim. Acta* **222**, 319–339 (2018).
131. Baker, D.R. & Moretti, R., Modeling the solubility of sulfur in magmas: a 50-year old geochemical challenge. *Rev. Mineral. Geochem.* **73**, 167–213 (2011).
132. Genda, H. & Abe, Y., Enhanced atmospheric loss on protoplanets at the giant impact phase in the presence of oceans. *Nature* **433**, 842–844 (2005).
133. Honda, M., McDougall, I., Patterson, D.B., Dougeris, A., & Clague, D.A., Possible solar noble-gas component in Hawaiian basalts. *Nature* **349**, 149 (1991).
134. Sarda, P., Staudacher, T., & Allègre, C.J., Neon isotopes in submarine basalts. *Earth Planet. Sci. Lett.* **91**, 73–88 (1988).
135. Mizuno, H., Nakazawa, K., & Hayashi, C., Dissolution of the primordial rare gases into the molten Earth's material. *Earth Planet. Sci. Lett.* **50**, 202–210 (1980).
136. Yokochi, R. & Marty, B., A determination of the neon isotopic composition of the deep mantle. *Earth Planet. Sci. Lett.* **225**, 77–88 (2004).
137. Lynne, A.H., Disk-dispersal and planet-formation timescales. *Phys. Scripta* **2008**, 014024 (2008).
138. Yin, Q. et al., A short timescale for terrestrial planet formation from Hf–W chronometry of meteorites. *Nature* **418**, 949 (2002).
139. Tang, H. & Dauphas, N.,  $^{60}\text{Fe}$ – $^{60}\text{Ni}$  chronology of core formation in Mars. *Earth Planet. Sci. Lett.* **390**, 264–274 (2014).
140. Rose-Weston, L., Brenan, J.M., Fei, Y., Secco, R.A., & Frost, D.J., Effect of pressure, temperature, and oxygen fugacity on the metal-silicate partitioning of Te, Se, and S: implications for earth differentiation. *Geochim. Cosmochim. Acta* **73**, 4598–4615 (2009).
141. Zhang, Y. & Yin, Q.-Z., Carbon and other light element contents in the Earth's core based on first-principles molecular dynamics. *Proc. Natl Acad. Sci.* **109**, 19579–19583 (2012).
142. Suer, T.-A., Siebert, J., Remusat, L., Menguy, N., & Fiquet, G., A sulfur-poor terrestrial core inferred from metal–silicate partitioning experiments. *Earth Planet. Sci. Lett.* **469**, 84–97 (2017).
143. Tsybulov, L.B. & Tsmekhman, L.S., Solubility of carbon in sulfide melts of the system Fe–Ni–S. *Russ. J. Appl. Chem.* **74**, 925–929 (2001).
144. Stolper, E., Fine, G., Johnson, T., & Newman, S., Solubility of carbon dioxide in albitic melt. *Am. Mineral.* **72**, 1071–1085 (1987).
145. Duncan, M.S. & Dasgupta, R., Pressure and temperature dependence of  $\text{CO}_2$  solubility in hydrous rhyolitic melt – implications for carbon transfer to mantle source of volcanic arcs via partial melt of subducting crustal lithologies. *Contrib. Mineral. Petrol.* **169**, 1–19 (2015).



146. Eguchi, J. & Dasgupta, R., A CO<sub>2</sub> solubility model for silicate melts from fluid saturation to graphite or diamond saturation. *Chem. Geol.* **487**, 23–38 (2018).
147. Behrens, H., Ohlhorst, S., Holtz, F., & Champenois, M., CO<sub>2</sub> solubility in dacitic melts equilibrated with H<sub>2</sub>O–CO<sub>2</sub> fluids: implications for modeling the solubility of CO<sub>2</sub> in silicic melts. *Geochim. Cosmochim. Acta* **68**, 4687–4703 (2004).
148. Duncan, M.S. & Dasgupta, R., Rise of Earth's atmospheric oxygen controlled by efficient subduction of organic carbon. *Nat. Geosci.* **10**, 387–392 (2017).
149. Stolper, E. & Holloway, J.R., Experimental determination of the solubility of carbon dioxide in molten basalt at low pressure. *Earth Planet. Sci. Lett.* **87**, 397–408 (1988).
150. Pan, V., Holloway, J.R., & Hervig, R.L., The pressure and temperature dependence of carbon dioxide solubility in tholeiitic basalt melts. *Geochim. Cosmochim. Acta* **55**, 1587–1595 (1991).
151. Yoshioka, T., McCammon, C.A., Shcheka, S., & Keppler, H., The speciation of carbon monoxide in silicate melts and glasses. *Am. Mineral.* **100**, 1641–1644 (2015).
152. Wetzel, D.T., Rutherford, M.J., Jacobsen, S.D., Hauri, E.H., & Saal, A.E., Degassing of reduced carbon from planetary basalts. *Proc. Natl Acad. Sci.* **110**, 8010–8013 (2013).
153. Dasgupta, R., Hirschmann, M.M., & Smith, N.D., Partial melting experiments of peridotite + CO<sub>2</sub> at 3 GPa and genesis of alkalic ocean island basalts. *J. Petrol.* **48**, 2093–2124 (2007).
154. Mallik, A. & Dasgupta, R., Effect of variable CO<sub>2</sub> on eclogite-derived andesite-lherzolite reaction at 3 GPa – implications for mantle source characteristics of alkalic ocean island basalts. *Geochem. Geophys. Geosyst.* **15**, 1533–1557 (2014).
155. Vetere, F., Holtz, F., Behrens, H., Botcharnikov, R.E., & Fanara, S., The effect of alkalis and polymerization on the solubility of H<sub>2</sub>O and CO<sub>2</sub> in alkali-rich silicate melts. *Contrib. Mineral. Petrol.* **167**, 1014 (2014).
156. Ghiorso, M.S. & Gualda, G.A.R., An H<sub>2</sub>O–CO<sub>2</sub> mixed fluid saturation model compatible with rhyolite-MELTS. *Contrib. Mineral. Petrol.* **169**, 53 (2015).
157. Stanley, B.D., Hirschmann, M.M., & Withers, A.C., Solubility of C–O–H volatiles in graphite-saturated martian basalts. *Geochim. Cosmochim. Acta* **129**, 54–76 (2014).
158. Wade, J. & Wood, B.J., Core formation and the oxidation state of the Earth. *Earth Planet. Sci. Lett.* **236**, 78–95 (2005).
159. Rubie, D.C. et al., Heterogeneous accretion, composition and core–mantle differentiation of the Earth. *Earth Planet. Sci. Lett.* **301**, 31–42 (2011).
160. Badro, J., Brodholt, J.P., Piet, H., Siebert, J., & Ryerson, F.J., Core formation and core composition from coupled geochemical and geophysical constraints. *Proc. Natl Acad. Sci.* **112**, 12310–12314 (2015).
161. Okuchi, T., Hydrogen partitioning into molten iron at high pressure: implications for Earth's core. *Science* **278**, 1781–1784 (1997).
162. O'Neill, H.S.C., The origin of the moon and the early history of the earth – a chemical model. Part 2: the earth. *Geochim. Cosmochim. Acta* **55**, 1159–1172 (1991).
163. Kleine, T. et al., Hf–W chronology of the accretion and early evolution of asteroids and terrestrial planets. *Geochim. Cosmochim. Acta* **73**, 5150–5188 (2009).
164. Rubie, D.C. et al., Accretion and differentiation of the terrestrial planets with implications for the compositions of early-formed Solar System bodies and accretion of water. *Icarus* **248**, 89–108 (2015).

165. Canup, R.M. & Asphaug, E., Origin of the Moon in a giant impact near the end of the Earth's formation. *Nature* **412**, 708 (2001).
166. Čuk, M. & Stewart, S.T., Making the Moon from a fast-spinning Earth: a giant impact followed by resonant despinning. *Science* **338**, 1047–1052 (2012).
167. Deguen, R., Olson, P., & Cardin, P., Experiments on turbulent metal–silicate mixing in a magma ocean. *Earth Planet. Sci. Lett.* **310**, 303–313 (2011).
168. Deguen, R., Landeau, M., & Olson, P., Turbulent metal–silicate mixing, fragmentation, and equilibration in magma oceans. *Earth Planet. Sci. Lett.* **391**, 274–287 (2014).
169. Wohlers, A. & Wood, B.J., A Mercury-like component of early Earth yields uranium in the core and high mantle  $^{142}\text{Nd}$ . *Nature* **520**, 337–340 (2015).
170. Wohlers, A. & Wood, B.J., Uranium, thorium and REE partitioning into sulfide liquids: implications for reduced S-rich bodies. *Geochim. Cosmochim. Acta* **205**, 226–244 (2017).
171. Münker, C., Fonseca, R.O.C., & Schulz, T., Silicate Earth's missing niobium may have been sequestered into asteroidal cores. *Nat. Geosci.* **10**, 822 (2017).
172. Wade, J. & Wood, B.J., The oxidation state and mass of the Moon-forming impactor. *Earth Planet. Sci. Lett.* **442**, 186–193 (2016).
173. Krasnokutski, S.A. et al., Low-temperature condensation of carbon. *Astrophys. J.* **847**, 89 (2017).
174. Li, Y., Marty, B., Shcheka, S., Zimmermann, L., & Keppler, H., Nitrogen isotope fractionation during terrestrial core–mantle separation. *Geochem. Perspect. Lett.* **2**, 138–147 (2016).
175. Labidi, J. et al., Experimentally determined sulfur isotope fractionation between metal and silicate and implications for planetary differentiation. *Geochim. Cosmochim. Acta* **175**, 181–194 (2016).